



Cite this: *Environ. Sci.: Adv.*, 2025, 4, 1279

## Sustainability driven additive manufacturing: repetitive mechanical recycling response evaluation to valorize polycarbonate scrap†

Markos Petousis,<sup>a</sup> Nikolaos Michailidis,<sup>bc</sup> Vassilis Papadakis,<sup>de</sup> Katerina Gkagkanatsiou,<sup>a</sup> Apostolos Argyros,<sup>id bc</sup> Nikolaos Mountakis,<sup>a</sup> Vasileios Stratiotou Efstratiadis,<sup>bc</sup> Constantine David,<sup>f</sup> Dimitrios Sagris<sup>f</sup> and Nectarios Vidakis<sup>id \*a</sup>

Polycarbonate (PC) is a widely used thermoplastic. Therefore, the amount of waste produced is notable. The exploitation of such waste is of great interest nowadays in the industry and academic society, due to its contribution to environmental pollution and other negative consequences. Herein, the possibility of using PC scrap as a raw material in 3D printing (material extrusion – MEX) is reported. The efficacy of the PC polymer after six thermomechanical courses was evaluated. The effect on rheology, mechanical performance, and thermal behavior is reported. The morphological characteristics were also assessed through scanning electron microscopy, while two quality metrics, *i.e.*, geometrical accuracy and 3D printing structure porosity of the parts, were investigated through micro-computed tomography. The findings were correlated to report the impact of thermomechanical processing on the PC polymer properties. A 9% tensile strength increase compared to the virgin polymer is reported (third round), while the flexural strength was improved by 14% (second round). Then the strength declined. It was lower than that of the virgin material on the sixth thermomechanical repetition. The findings showed that the life of PC can be extended through thermomechanical recycling for 3D printing applications.

Received 22nd February 2025  
Accepted 16th June 2025

DOI: 10.1039/d5va00048c

rsc.li/esadvances

### Environmental significance

The recycling of polycarbonate in 3D printing reduces dependence on virgin resources, mitigates environmental impact, and presents a sustainable solution to the issue of plastic waste. This research demonstrates that polycarbonate waste can be converted into high-quality filaments for 3D printing, thereby promoting a circular economy. This approach reduces carbon footprint and resource depletion by circumventing the disposal of plastic in landfills and avoiding energy-intensive production processes. The results support the adoption of responsible manufacturing practices, which contribute to waste reduction and facilitate environmentally sustainable additive manufacturing. This study has demonstrated that addressing plastic pollution necessitates the development of innovative recycling strategies for both industrial and consumer applications, exploiting 3D printing advantages, when polymers reach the end of their life.

## 1. Introduction

Additive manufacturing (AM) (commonly referred to as three-dimensional printing (3D-P)), is initially presented as a prototyping technology that has been developed into a technique for the production of final everyday products.<sup>1–4</sup> There is great interest in 3D printing, which has led to investigating the 3D fabricated parts' properties and behavior.<sup>5</sup> Efforts are made by AM to manufacture parts with the necessary characteristics that are as optimum as possible. For example, complex geometries,<sup>6</sup> flexibility,<sup>7</sup> and cost-effectiveness have been investigated.<sup>8</sup> In this direction, efforts are being made to improve the properties of the utilized materials.<sup>9</sup> The main AM applications and materials utilized are summarized in Table 1.

The idea of sustainable manufacturing needs to be adopted by the global plastics industry for as many plastics as possible<sup>52</sup>

<sup>a</sup>Department of Mechanical Engineering, Hellenic Mediterranean University, Heraklion 71410, Greece. E-mail: markospetousis@hmu.gr; gkagka@hmu.gr; mountakis@hmu.gr; vidakis@hmu.gr; Tel: +30 2810379227

<sup>b</sup>Physical Metallurgy Laboratory, Mechanical Engineering Department, School of Engineering, Aristotle University of Thessaloniki, 54124 Thessaloniki, Greece. E-mail: nmichail@auth.gr; aargyros@auth.gr; vstratio@meng.auth.gr

<sup>c</sup>Centre for Research & Development of Advanced Materials (CERDAM), Center for Interdisciplinary Research and Innovation, Balkan Centre, Building B', 10th km Thessaloniki-Thermi Road, 57001, Thessaloniki, Greece

<sup>d</sup>Department of Industrial Design and Production Engineering, University of West Attica, 122 44 Athens, Greece. E-mail: v.papadakis@uniwa.gr

<sup>e</sup>Institute of Electronic Structure and Laser of the Foundation for Research and Technology-Hellas (IESL-FORTH), N. Plastira 100, 70013 Heraklion, Greece

<sup>f</sup>Department of Mechanical Engineering, International Hellenic University, Serres Campus, 62124, Greece. E-mail: david@ihu.gr; dsagris@ihu.gr

† Electronic supplementary information (ESI) available. See DOI: <https://doi.org/10.1039/d5va00048c>



Table 1 Summary of the AM applications and materials utilized

| Applications of AM                    | AM materials             | AM polymers  |
|---------------------------------------|--------------------------|--|
| Automotive <sup>10</sup>              | Resins <sup>11</sup>     | Polylactic acid (PLA) <sup>12–14</sup>                 |
| Aerospace <sup>15–21</sup>            | Metals <sup>22</sup>     | Polycarbonate (PC) <sup>23,24</sup>                    |
| Medicine <sup>25–28</sup>             | Ceramics <sup>29</sup>   | Acrylonitrile butadiene styrene (ABS) <sup>30–33</sup> |
| Scientific equipment <sup>34–36</sup> | Thermoplastics           | High-density polyethylene (HDPE) <sup>37</sup>         |
| Biomedicals, energy <sup>38</sup>     | Polymer blends           | Polyamide <sup>39</sup>                                |
| Construction <sup>40,41</sup>         | Composites               | Polyetheretherketone (PEEK) <sup>42</sup>              |
| Electronics <sup>43–46</sup>          | Thermosets <sup>47</sup> | Other <sup>48–51</sup>                                 |

by adopting a recyclable economy.<sup>53,54</sup> The environmental issues, protection of resources, and limiting of the scrap material need to be given attention, which is the reason why polymer reprocessing is highly attempted by plastic-converting industries.<sup>55–57</sup> In this direction, the mechanical behavior of recycled polymeric parts has attracted the scientific community's attention.<sup>58</sup>

Life cycle assessment (LCA) is a method of assessing the environmental performance of products and preventing pollution during the stages of their life cycle.<sup>59</sup> Various environmental issues can be limited by following LCA during the creation of optimized products characterized by environmental sustainability.<sup>60,61</sup> The global plastics industry has been studying this concept in several investigations,<sup>62,63</sup> including those related to plastic losses from seafood supply chains.<sup>64</sup>

One of the most widely consumed engineering plastics is PC, which holds an important position in many fields owing to its desirable properties. Some of them have high transparency,<sup>65,66</sup> thermal stability,<sup>67,68</sup> thermal and flame resistance,<sup>69</sup> and high impact-strength stability under alternating environmental conditions.<sup>70,71</sup> The aforementioned characteristics make PC suitable for industrial applications, such as building, medical,<sup>72,73</sup> automotive, transportation, construction, electrical applications,<sup>74,75</sup> and optical and technical applications.<sup>69</sup> In particular, it is useful for producing bulletproof windows, food packaging, optical devices, and water bottles.<sup>76,77</sup> Moreover, to achieve lightweight properties in electric vehicles, sustainability is a critical aspect, providing a solution for electric vehicle range issues.<sup>78</sup> It is also useful as the primary manufacturing material in the case of some 5G apparatus.<sup>79</sup>

According to information provided in the available market reports, in 2021 the global PC market was measured to be USD 19.6 billion. Between 2022 and 2031, the compound annual growth rate (CAGR) is estimated to be 6.2%, meaning that the global PC market would be USD 37.99 billion by the end of 2031.<sup>80</sup> The value of the global PC market size was USD 22,594.10 million in 2022 and a 3.5% CAGR is expected between 2023 and 2030.<sup>81</sup> In an additional report,<sup>82</sup> it is stated that the global PC market in 2023 was valued at about 15.11 billion and forecasted to grow between the 2023–2032 period, from 15.86 billion to 24.31 billion, with a CAGR of 5.4%. Based on another<sup>83</sup> report, the recycled polycarbonate market size in 2023 was calculated to be approximately USD 101 billion. By 2030, it is estimated that the number will become USD 174.7 billion, with a 6.5% CAGR for the 2024–2030 period. Moreover, in another<sup>84</sup>

report, the global PC market size in 2023 was USD 20.80 billion, and it was estimated that by 2033, it would reach USD 36.84 billion. The CAGR was calculated to be approximately 5.68% for the 2024–2033 forecast period. In another<sup>85</sup> report, the global PC thermoplastic market in the year 2022 was estimated at USD 21.75 billion, with a CAGR being 5.90% between 2022 and 2030 and anticipation of USD 32.36 billion being reached by 2030.

Such an extension is expected to lead to the generation of large amounts of PC waste when it reaches its end of life. Therefore, recycled polycarbonate (PC) has emerged as a key research topic in attempts to promote sustainable development and a circular economy, especially regarding polymeric materials; because of the large amount of waste and emissions, they are now essential for current applications.<sup>86</sup> PC was examined for its performance after recycling by the end of its first life cycle.<sup>87,88</sup> The results indicate a severe reduction in the physical and mechanical properties caused by the recycling process.<sup>89</sup> Research has been conducted on PC,<sup>90</sup> the formation of composites,<sup>91</sup> the application of PC polymer recycling technologies,<sup>92</sup> and its environmental impact.<sup>93,94</sup> PC-based nanocomposites have been examined in relation to their behavior and how they are influenced by recycling.<sup>95,96</sup>

Pure PC has also been studied to examine the impact of the recycling course on its properties, in the study by Pérez *et al.*,<sup>97</sup> where it was proved that over ten cycles of recycling causes a reduction of tensile strength by 30%. In the study of Bernardo *et al.*,<sup>98</sup> the impact of recycling on the mechanical performance of fiber-reinforced PC was investigated. The results confirmed that its structure and properties were dependent on the thermomechanical recycling environment for the process (temperature, shear rate, and pressure). Additionally, the PC polymer's molecular weight, moisture content, and the nature of the additives are vital. Although in 3D printing (MEX method) the mechanical response of the PC thermoplastic has been presented,<sup>24,99,100</sup> and compounds have been formed, using it as the matrix polymer,<sup>101–103</sup> its response when recycled with the thermomechanical extrusion process has not been reported yet, according to the bibliography found. Still, its use as a virgin material in eco-friendly applications has been investigated.<sup>104</sup> Recycled polymers, such as ABS,<sup>105</sup> polypropylene (PP),<sup>106</sup> polyamide 12,<sup>107</sup> HDPE,<sup>108</sup> thermoplastic polyurethane (TPU),<sup>109</sup> and polyethylene terephthalate glycol (PETG),<sup>110</sup> have been investigated, by applying the thermomechanical reprocessing scenario with six successive courses, for use in MEX 3D printing. The findings show good potential for these polymers to be used in



3D printing applications at the end of their life, extending and contributing to the circular economy and their sustainability.

Considering the aforementioned information, the aim of this research was to report the level and type of influence that several recycling courses would have on the performance of PC made through 3D-P. The fabricated samples were examined after up to six thermal processing cycles. Mechanical recycling of PC is the main topic of this study, which also examines the impact of numerous recycling cycles on the structural, mechanical, thermal, and rheological characteristics. This study specifically attempted to evaluate PCs' longevity and performance, following six recycling cycles. Each cycle involves breaking the material into pieces, forming them into filaments, and then using 3D printing to create test specimens.<sup>111</sup> To determine how each recycling step affects the polymer integrity and usability in subsequent applications, these specimens subsequently underwent a variety of tests, including flexural, tensile, impact, and thermal examinations.<sup>112</sup> The samples were mechanically tested using flexural, tensile, Vickers microhardness, and Charpy impact strength tests. Dynamic mechanical analysis (DMA) was also performed. Thermal examinations included differential scanning calorimetry (DSC) and thermogravimetric analysis (TGA). The structural investigation was based on micro-computed tomography ( $\mu$ -CT) results regarding porosity and dimensional deviation. The morphological response was evaluated utilizing the technology of scanning electron microscopy (SEM) at several magnifications.

The goal of this study is to provide a thorough assessment of the recyclability of PCs and draw attention to the difficulties related to polymer deterioration over several cycles by examining characteristics such as tensile strength, flexural modulus, impact resistance, and thermal stability.<sup>113</sup>

The motivation to investigate recycled polycarbonate (PC) for MEX 3D printing stems from the growing demand for environmentally sustainable materials in AM, prompted by rising environmental concerns and material consumption. Polycarbonate, an engineering thermoplastic, is distinguished by its exceptional mechanical properties, toughness, and heat resistance, rendering it a promising high-performance material for 3D printing. However, the production of virgin PC is energy-intensive and dependent on fossil inputs, resulting in a considerable environmental impact. Simultaneously, the accumulation of PC waste from consumer products such as optical media, electronics, and packaging presents a significant environmental challenge. Recycling this waste into functional 3D printing filaments not only prevents plastic waste from polluting the environment but also diminishes the demand for virgin polymer production. Despite its potential, the incorporation of recycled PC into MEX 3D printing is currently impeded by concerns regarding material degradation, printability, and property retention. This research seeks to address these challenges through systematic investigation, thereby facilitating the adoption of recycled PC in AM without compromising functionality. By enhancing the understanding of recycled PC's performance in MEX printing, this study contributes to broader efforts toward circular economy approaches and sustainable manufacturing technology.

In addition to offering insightful information about the reusability of PCs, this study advances the conversation on sustainable polymer recycling methods with the goal of enhancing recycling procedures for better waste management and resource conservation.<sup>114,115</sup> The literature investigation did not reveal any similar research on the recycling of PC thermoplastic with a thermomechanical process in AM. The novelty presented in this research pertains to the development and characterization of an environmentally sustainable filament derived from recycled PC for application in MEX 3D printing. While virgin PC is acclaimed for its superior thermal stability and mechanical strength, its high cost and environmental impact limit its widespread utilization. Conversely, recycled PC offers a sustainable and cost-effective alternative; however, its application in MEX 3D printing has not been extensively investigated due to challenges associated with material degradation, printability, and consistency. This research addresses these challenges by implementing a controlled mechanical recycling process to produce high-quality PC filaments from post-consumer waste and optimizing critical printing parameters to achieve dimensional stability and interlayer adhesion in MEX 3D printing. Furthermore, comprehensive thermal, rheological, and mechanical characterization studies are conducted to assess the performance of the recycled PC filament in comparison to its virgin counterpart. The findings indicate that recycled PC can match or even overcome the performance of virgin PC while significantly reducing material costs and environmental impact. Consequently, this study advances the principles of a circular economy in additive manufacturing by establishing the technical feasibility and sustainability benefits of utilizing recycled engineering thermoplastics in FFF 3D printing processes. Therefore, the findings have merit for the sustainability of the PC polymer and the AM manufacturing method, the extension of the PC polymer life through recycling, and the contribution to the circular economy efforts. Through the process followed, it was proven that MEX 3D printing can be an efficient method for the reuse of the thermoplastic PC in respective applications even when it is reprocessed up to six times, without critical decline in its properties.

## 2. Materials and methods

Fig. 1 shows the preparation of the raw materials used in the experiments. In addition, the mechanical recycling strategy followed herein is presented. The mechanical recycling strategy applied in the present work, consisting of basic recycling steps, is as follows: weighing and drying the material before processing the raw material through the extruder to make the filament. Weighing of the sheets was carried out to keep track of how much raw material was used at each stage of the recycled process. It was part of the internal material handling and didn't affect the experiments themselves. After drying, the filament was used to prepare the specimens using the additive manufacturing method (MEX). The parts were then evaluated by mechanical, rheological, thermal, and morphological testing before their shredding for the next recycling course. This was repeated six times. Each step included two thermomechanical





Fig. 1 The steps followed in this research and the mechanical recycling strategy for the PC polymer. On the right side, the flow diagram of the process is depicted, and on the left side, corresponding screenshots for each step are shown.

processes, one for the filament and one for the specimens' production. The repetitions stopped at the sixth one, as the mechanical properties of the examples were already lower than the corresponding virgin material examples. Additionally, this was in agreement with the existing bibliography for polymer recycling in MEX 3D printing, presented above.<sup>105–110</sup>

## 2.1 Materials

The material chosen for this research was a polycarbonate solid 4 mm sheet, sourced from Isik Plastik, type Policam (Kocaeli Turkey,  $1.2 \text{ g cm}^{-3}$  density – ISO 1183, tensile strength  $> 60 \text{ MPa}$  – ISO 527, Vicat temperature at 50 N,  $50 \text{ }^\circ\text{C}$ ,  $148 \text{ }^\circ\text{C}$  – ISO 306). The shredded sheet was placed in a laboratory oven to dehydrate for a specific amount of time ( $60 \text{ }^\circ\text{C}$ , 12 h (ref. 99)), before being put into an extruder for filament production (1.75 mm). The filament measurements must be specific so that the diameter cannot cause problems in the MEX 3D printing process.

## 2.2 Recycling process

After the PC weighing and drying process, the material remnant sheet was taken and cut into pieces that were later placed in a shredder machine to produce pellets of the material. Afterward, the pellets were placed in a 3Devo 450 Precision (Utrecht, Netherlands) extruder for filament production.

The extrusion parameters were optimized based on the recommended settings provided by the extruder manufacturer (3Devo) and from this research group's previous research on PC processing in MEX 3D printing.<sup>116</sup> These helped define suitable temperature zones, screw speed, and cooling conditions for consistent and stable filament production.

The filament was extruded in order to be compatible with the MEX 3D printer parameters (1.75 mm diameter). Prior to its use, the produced filament underwent quality inspection for the

consistency of its diameter, uniformity of its side surface, and its strength in tensile testing. The results are presented in the ESI† of the research.

The 3D printer machine used for the production of the parts was a MEX 3DP Intamsys Funmat HT from Shanghai, China. The specimens were manufactured to suit all the mechanical testing parameters. In Fig. 2, the set 3D printing settings, the initial design of the parts, and the international standards that were followed are presented. The first recycling cycle was conducted using this process, as well. The 3D printing parameters were selected based on extensive previous work on optimizing 3D printing settings for polycarbonate, and by consulting the respective literature,<sup>99,100</sup> which provided valuable insights into how printing temperature, speed, and cooling affect the quality and mechanical properties of printed PC parts.

It should be noted that PC is known for its warping issues in MEX 3D printing. Therefore, a 3D printing environment was set specifically to minimize such issues. This setup was tested and adjusted in preliminary tests, prior to building the samples for the current research. More specifically, the printer used (Intamsys Funmat HT) had the chamber set at  $90 \text{ }^\circ\text{C}$  and the bed at  $100 \text{ }^\circ\text{C}$ , which helped keep the temperature stable. These were the optimum temperatures found for this research. An adhesive was also used on the build plate for better first-layer grip. With these settings, warping was not observed in the 3D printed samples, as presented in the respective images of actual research samples below.

Following this process, in order to carry out the six recycling cycles, the already manufactured specimens were put into the shredder, so that they could become suitable for filament production. The pellets were then placed into the extruder to make the filament for subsequent cycles. The new filament was placed into a 3D printer to produce the parts. Later, these 3D printed parts (specimens) were mechanically, thermally, morphologically, and structurally tested in the same manner as



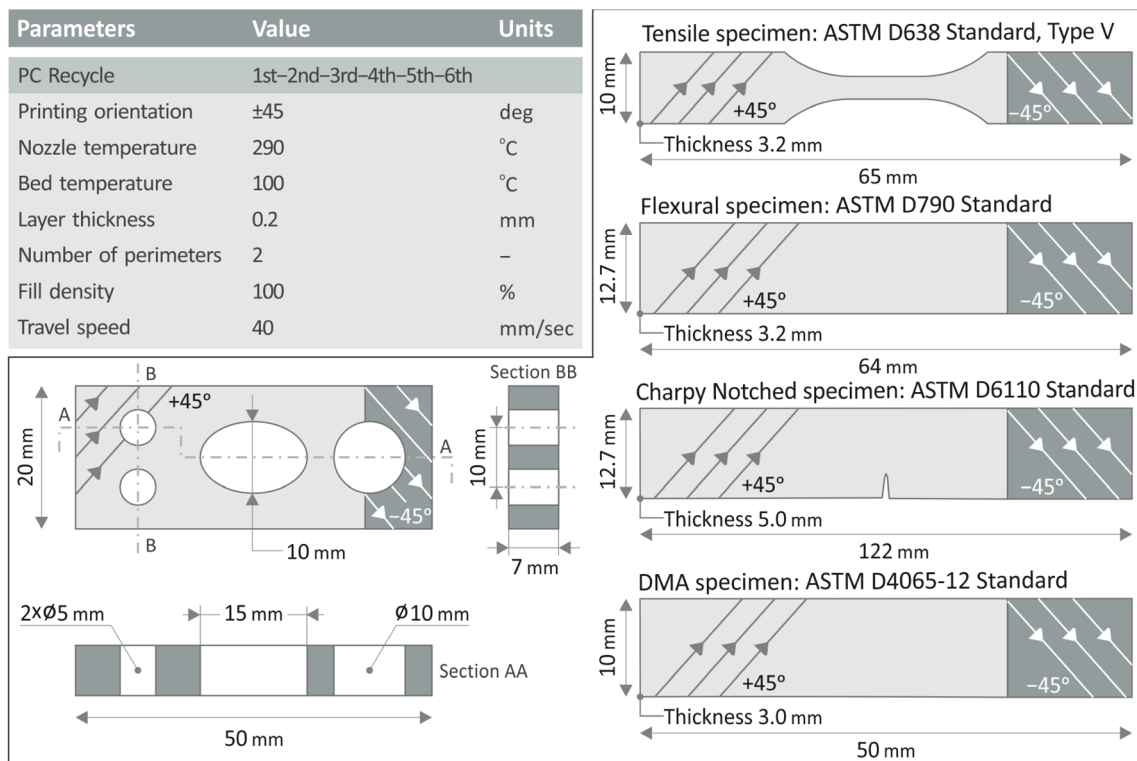


Fig. 2 List of 3D printing parameters, for the six recycling cycles, designs, dimensions, and international standards of the needed specimens.

the previous specimens. This process was repeated five times at the end of the experimental testing for each cycle (six recycling courses in total).

It should be noted that in every one of the six cycles, there were two different thermomechanical treatments. One is the fabrication of the filament and the other is the 3D printing process. For this work, the total amount of specimens created was one hundred and fifty. In each of the six cycles, there were five replicas for each test, *i.e.*, tensile, flexural, Charpy impact, and DMA mechanical tests. For this part of the research, the total amount was one hundred and twenty (120) specimens. Additionally, sixty  $\mu$ -CT checks were conducted in total in respective examples from each of the six cycles (30 on tensile samples for their 3D printing structure and 30 on the samples shown on the bottom left side of Fig. 2 for their dimensional accuracy). Furthermore, thirty SEM examinations were conducted on tensile samples after they were tested. Overall, there were 210 tests conducted in the research, whereas all the scanning and analysis files created a total of more than 100 gigabytes.

### 2.3 Mechanical examination

The specimens underwent five different mechanical tests, and each test was conducted following the respective ASTM standards. Tensile testing was carried out using an Imada model MX2 from Northbrook, Illinois, United States, following the instructions of ASTM D638-02a (3.2 mm thickness examples, type V, and a 10 mm  $\text{min}^{-1}$  elongation rate). Flexural testing

was performed on the same apparatus with the tensile experiments, following in this case the ASTM D790 Standard, with a 50.8 mm span and 10 mm  $\text{min}^{-1}$  elongation rate. The Charpy impact test was implemented on a model MT 220 by Terco, Kungens Kurva, Sweden, following the ASTM D4065-12 Standard, on notched samples with 367 release height. Vickers Microhardness, by an Innova Test, model 300 from Maastricht, Netherlands, following the ASTM E384-17, with 200 gF applied load and 10 s indentation duration. Dynamic mechanical analysis (DMA) testing employed the DHR20 Discovery Hybrid Rheometer (sourced from the TA Instruments company, established in New Castle, Delaware, United States). For the geometry setup, a span of 40 mm was adjusted for 3-point bending. The dimensions of the parts were 10 mm  $\times$  50 mm  $\times$  3 mm. DMA was carried out over the range of 30–200 °C at a heating step of 5 °C  $\text{min}^{-1}$ . Throughout the experiment, the apparatus applied sinusoidal strains oscillating at a frequency of 1 Hz, varying between 0 and 0.05%. A force-tracking system was employed to maintain continuous contact with the sample during the test.

### 2.4 Thermal examination

To examine the thermal properties and changes that occurred in the specimens in every cycle of the PC material, Thermogravimetric Analysis (TGA) was performed on the Discovery Simultaneous Thermal Analyzer SDT 650 of TA Instruments (capable of operating with a temperature range from room temperature to 1500 °C, a heating step of 0.1–100 °C  $\text{min}^{-1}$  and



a balance accuracy of  $\pm 0.5\%$ ), which operated within a temperature cycle starting at 25 °C, rising to 800 °C and equilibrating.<sup>117</sup>

Differential Scanning Calorimetry (DSC) was utilized to analyze the thermal response of the filaments. The tests were carried out utilizing a Discovery-Series DSC 25 apparatus (TA Instruments, Delaware, USA), equipped with a Cooling System (temperature range between  $-90$  and  $725$  °C and heating rates of  $0.01$ – $100$  °C  $\text{min}^{-1}$ ) which operated within a temperature cycle starting at 25 °C, rising to 300 °C, and then cooling back to 25 °C, at a rate of  $15$  °C  $\text{min}^{-1}$ .<sup>118</sup>

## 2.5 Rheological examination and MFR

Rheological measurements were carried out on all the filaments to evaluate the response of their viscosity to shear stress. A Discovery Hybrid Rheometer apparatus model DHR20 by the company TA Instruments, established in New Castle, Delaware, United States equipped with a parallel plate setup and a heating system that operates between  $-160$  and  $600$  °C was used for the analysis. This advanced measurement setup improved the sensitivity and accuracy, enabling the detection of lower viscosities while requiring less material.

The tests were conducted at 270 °C, similar to the nozzle temperature used for printing the first layer, with a torque range of  $1$ – $100\,000$   $\mu\text{N m}$  and a plate diameter of 25 mm with a 1 mm plate clearance of 120. Melt Flow Rate (MFR) evaluations were also used to analyze the flow behavior of the composites through an orifice of a specified length and diameter at controlled temperature (300 °C) and pressure, according to the ASTM D1238-13 standard.

## 2.6 Raman spectra

Raman spectra were acquired employing a LabRAM HR Raman Spectrometer, by the company HORIBA Scientific, established in Kyoto, Japan. The methodology and parameters are provided in the ESI† of the manuscript.

## 2.7 Morphological examination (SEM)

The failed tensile test examples were inserted into SEM to assess their morphological characteristics. An apparatus model named JSM 6362LV (by the JEOL company, located in Tokyo, Japan) was set in high vacuum mode at 20 kV. Prior to SEM scanning, the specimens were covered in Au to achieve a reduction in the charging effects while capturing the images. The lateral and fractured sides of the examples were analyzed at different magnifications.

## 2.8 Structural examination

To characterize the 3D printed parts structure, a scanning course of  $\mu$ -CT was carried out utilizing a Tomoscope Micro Focus CT-scanner model named HV Compact 225 kV from the company Werth Messtechnik GmbH, located in Gießen, Germany. Prior to mechanical testing, the internal structure of the 3D printed parts was investigated (16L scanning resolution), along with their geometric fidelity (60L scanning resolution). The scanning parameters for the ideal image quantity were set according to parameters, such as the material density of the specimens and their size. The software VG Studio MAX 2.2, from the company Volume Graphics GmbH, in Heidelberg, Germany was used for the quantitative and visual analysis of the

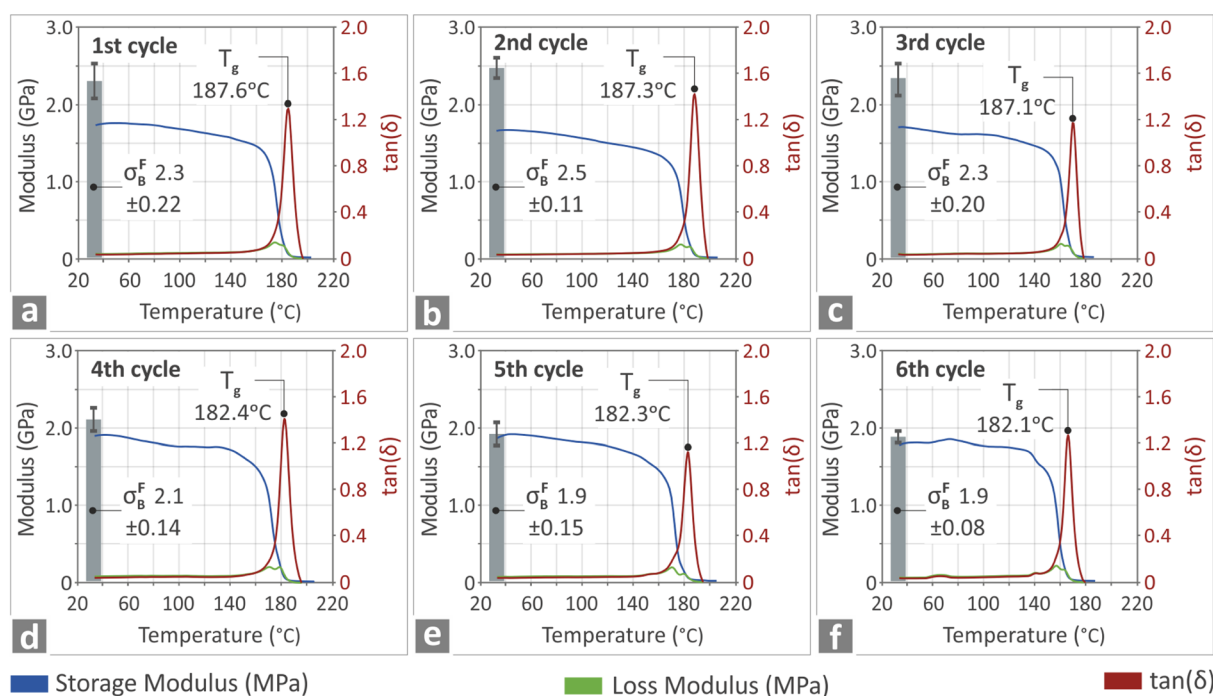


Fig. 3 DMA results in graphs of flexural modulus, loss and storage modulus,  $\tan(\delta)$  versus temperature modulus for every one of the six recycling cycles of PC. (a) 1st cycle, (b) 2nd cycle, (c) 3rd cycle, (d) 4th cycle, (e) 5th cycle, (f) 6th cycle.



reconstructed 3D geometry of the specimens in accordance with the CT data.

## 3. Results

### 3.1 Mechanical examination and DMA

Fig. 3 presents the outcome derived from DMA testing of the six PC recycling cycles. For the PC remnant (Fig. 3a–f), graphs with reference to the temperature of the loss and storage modulus, and  $\tan(\delta)$  are displayed. The existing bar on each graph represents the flexural modulus of elasticity in each cycle (which is displayed in more detail in Fig. 5) for comparison with the respective storage modulus. It can be observed that in every cycle, the storage modulus decreases steadily, whereas the loss modulus and  $\tan(\delta)$  decrease when they reach the  $T_g$  temperature and then decrease. This occurred at approximately 180 °C.

Fig. 3a–f display as functions of temperature the storage and loss moduli and loss factor  $\tan(\delta)$ , along with  $T_g$  for all six samples, at each recycling cycle. The storage modulus presents a relatively steady trend among the samples, with the highest value being that of the 2<sup>nd</sup> recycling cycle samples (Fig. 3b). The loss modulus remained low and steady throughout the experiments. As for  $\tan(\delta)$ , the trend is similar among the samples, with the highest value being that of the 2<sup>nd</sup> recycling cycle sample (Fig. 3b), whereas  $T_g$  (maximum of  $\tan(\delta)$ ) presents a decreasing trend, which is in accordance with the DSC analysis.

In Fig. 4–6, the mechanical test results, which were conducted on samples of every one of the six recycling cycles, are graphically presented. Fig. 4a presents the tensile strength, Fig. 4b presents the tensile modulus of elasticity, and Fig. 4c presents the tensile toughness. The samples of the third recycling cycle present the highest results of tensile toughness and

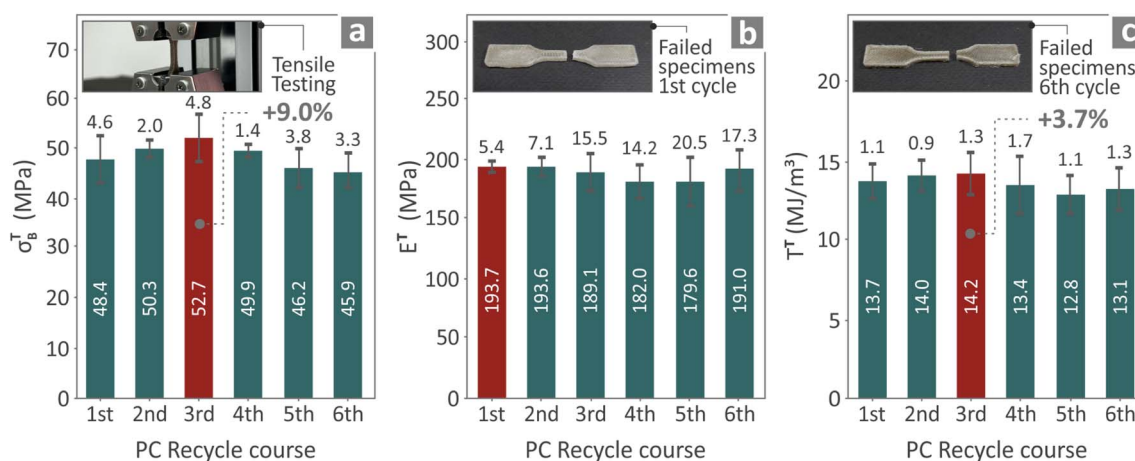


Fig. 4 The tensile properties of the samples from the six PC recycling courses are presented. In detail, (a)  $\sigma_b^T$  results accompanied by an image during the testing, (b)  $E^T$  results accompanied by an image of the tested specimens of the first cycle and (c)  $T^T$  results accompanied by an image of the tested specimens of the sixth cycle.

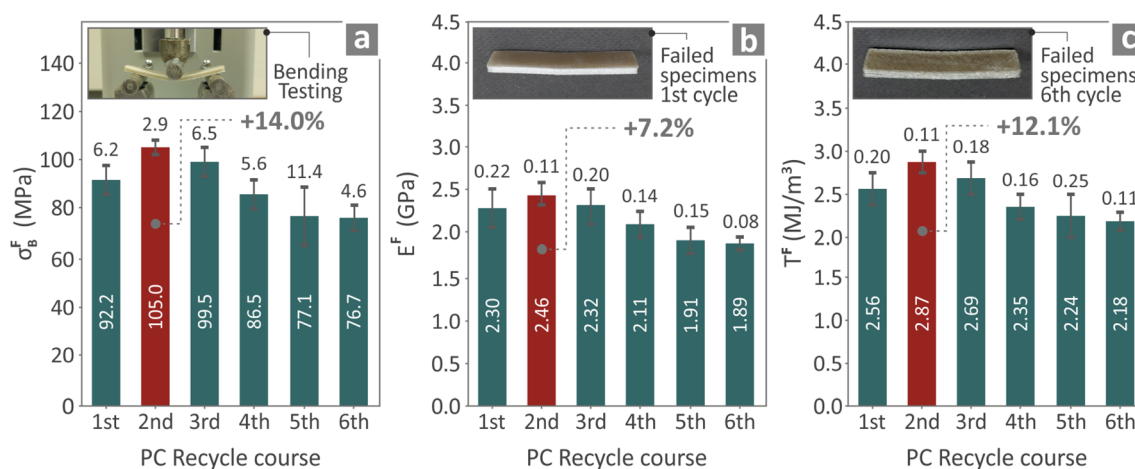


Fig. 5 The flexural properties of the tested flexural specimens from the six PC recycling cycles are presented namely (a) the  $\sigma_b^F$  (flexural strength) outcome accompanied by an image from the testing, (b)  $E^F$  (flexural modulus) outcome and image from the first course's tested specimens, and (c)  $T^F$  (flexural toughness) outcome accompanied by an image from the tested specimens of the sixth cycle.



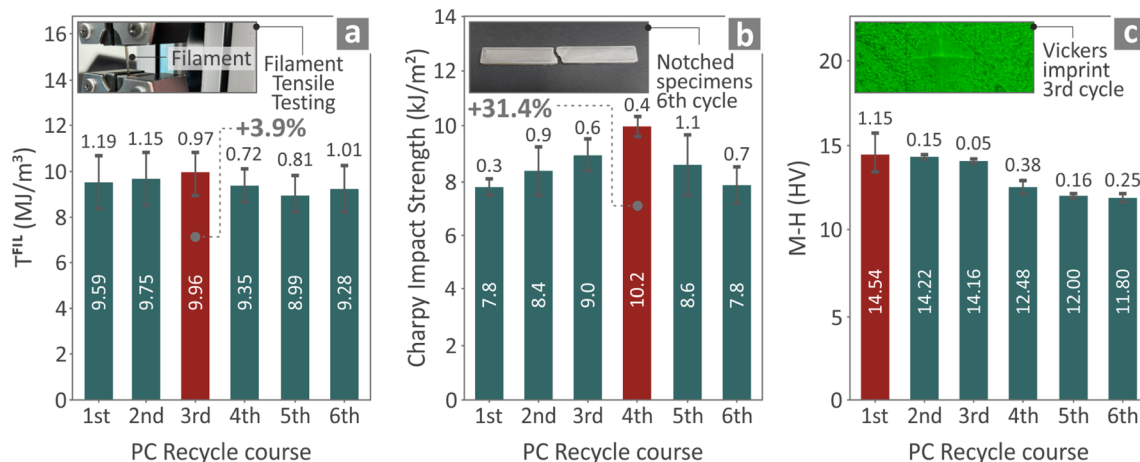


Fig. 6 Results from the samples tested from every recycling cycle of the PC. (a) Filament toughness  $T^{FIL}$ , (b) impact strength (Charpy), and (c) M-H measurements on samples, all accompanied by images captured during the testing procedures.

strength, compared to the other cycles, with a rise of +9.0% and +3.7%, respectively, while for the Young modulus, the highest results were obtained in the first cycle. This indicates that the stiffness of the PC material reduces with successive thermo-mechanical processing. In addition, Fig. 4a shows an image taken during tensile mechanical testing, and Fig. 4b and c show images from the already tested tensile specimens from the first and sixth recycling cycles.

Fig. 5a shows the flexural strength, Fig. 5b presents the modulus of elasticity in the flexural test, and Fig. 5c presents the flexural toughness. It is depicted that the tested specimens from the second recycling cycle had the highest results among the rest of the cycles, by +14.0%, +7.2%, and +12.1%, respectively. Fig. 5a shows an image during flexural testing on a random sample, and Fig. 5b and c include images from the tested flexural specimens of the first and sixth recycling cycles.

Fig. 6a displays the toughness results of the filaments, including an image from the respective experimental process (tensile testing). Fig. 6b shows the Charpy impact strength results, including an image of a notched specimen from the sixth cycle. Fig. 6c presents the M-H results while showing an image of the Vickers process of the third cycle. As can be observed from the toughness values for the filaments (Fig. 6a), the samples from the third recycling cycle presented the highest value among the rest of the cycles, by +3.9% compared to the first cycle. This outcome shows a trend which agrees with the tensile test on the 3D printed examples, still, the difference is within the statistical error. The Charpy impact results showed an improvement of +31.4% from the fourth cycle above the first cycle. The M-H examination results of the first cycle were the highest compared to those of the other cycles. This finding suggests that apart from the stiffness, the hardness of the PC thermoplastic also reduces, with the increase of thermo-mechanical processing.

### 3.2 Thermal examination

Fig. 7 presents the findings of the thermal examination of the six PC recycling cycles. Fig. 7a and b present the TGA analysis

and the Initial Decomposition Temperature (IDT) of 95%, the temperature at which 5% of the material mass has been lost due to thermal decomposition, and the Fractional Residue (%) (FR) after thermal degradation results, respectively. In the DSC analysis, as shown in Fig. 7b and c, the glass transition temperature ( $T_g$ ) of the recycled samples did not change significantly (<3%) but slightly decreased with each recycling cycle.

### 3.3 Rheological examination and MFR

In the rheological analysis of the six polycarbonate samples subjected to successive recycling cycles (ranging from one to six cycles of recycling), as shown in Fig. 8a, a progressive reduction in viscosity  $\eta$  with each additional recycling stage can be observed as the shear rate increases. Specifically, the first sample, which underwent only a single recycling, exhibited the highest viscosity, whereas the sixth sample, recycled six times, demonstrated the lowest viscosity. This reduction in viscosity can be attributed to the degradation of polymer chains during each recycling process.<sup>119</sup>

With repeated thermal and mechanical stresses during recycling, the molecular chains of polycarbonate can undergo scission, resulting in shorter molecular chain lengths and, consequently, a decrease in molecular weight. As the number of chain interactions decreased, the resistance of the polymer to flow weakened, resulting in a decrease in its viscosity.<sup>120</sup> All samples exhibited shear-thinning behavior. As expected, when the viscosity decreases, the sample flows more easily; hence, MFR presents an inversely proportional, progressively increasing MFR, as shown in Fig. 8b. The trend of the results solidifies the significance of the thermal and mechanical strain history of materials during recycling on their performance and applications.<sup>121</sup>

### 3.4 Raman spectroscopy

In Fig. 9a, the spectral profiles of the Raman analysis of PC are presented for every recycling cycle. Table 2 (presented below) shows the significant Raman peaks and their related



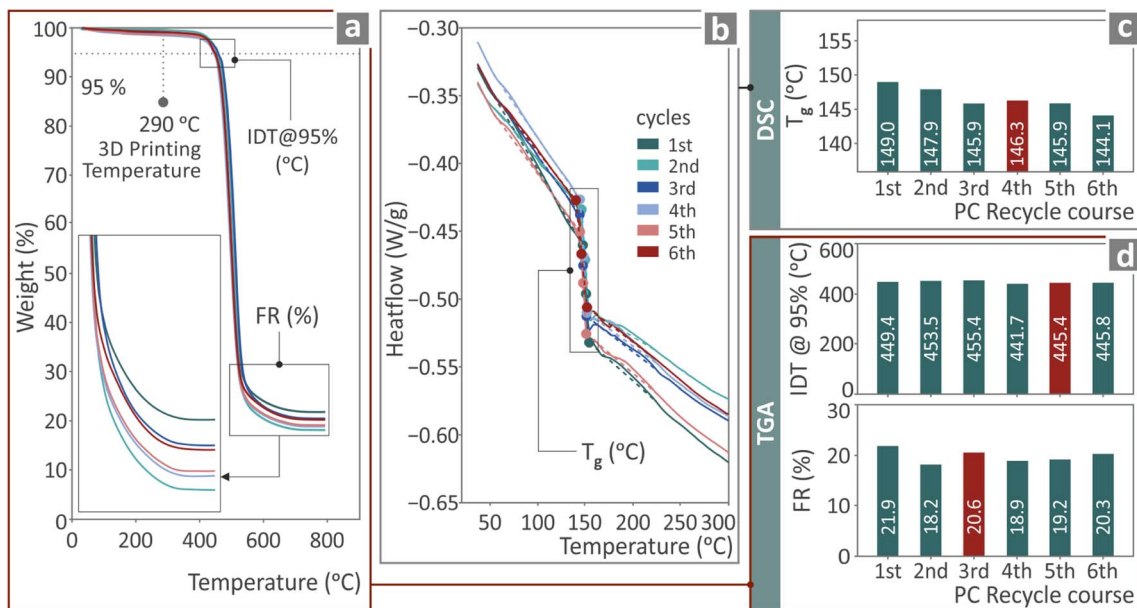


Fig. 7 The six PC recycling cycles samples, presenting: (a) the graphs of the TGA, (b) the DSC graphs, (c) the differential scanning calorimetry findings, and (d) the TGA findings.

assignments of the PC samples, as presented in the literature. Fig. 9b shows that the recycling cycles exhibited many spectral changes. We observed that the recycling cycles did not affect the Raman signal, and no significant or small changes were observed. In general, we observed only a small photoluminescence signal appearing in the first cycle.

### 3.5 Morphological examination (SEM)

Images captured during SEM analysis of the PC samples from various recycling cycles are included in Fig. 10. Images from the lateral side of the PC first, third, and sixth recycling cycle samples, magnified by 150 $\times$ , are presented in Fig. 10a–c, while Fig. 10g–i present the same images at 5000 $\times$  magnification. Fig. 10d–f display the fractured surface of the PC first, third, and sixth recycling cycle samples magnified in 27 $\times$  images. The

SEM analysis results of the second cycle samples are depicted in the illustrations in Fig. 11. Fig. 11c and d present the fractured surface enlarged in 27 $\times$ , 1000 $\times$  and 5000 $\times$ , respectively, while Fig. 11a and b present the lateral surfaces in 27 $\times$  and 150 $\times$  magnifications. According to the lateral surfaces' pictures, the layer distribution is excellent in all of the cycle samples. In the sixth cycle, some defects in the formation of the layers can be observed and other minor defects, indicating that the PC polymer behavior has been affected by the thermomechanical reprocessing. The fractured surfaces display primarily ductile behavior, with minimum deformation.

The SEM illustrations of the PC second-cycle examples are displayed in Fig. 11. Fig. 11a and b show the side surface findings at 27 $\times$  magnification, while Fig. 11c–e show the fractured surfaces at 27 $\times$ , 1000 $\times$ , and 5000 $\times$  magnification. The fractured surface images exhibited brittle behavior. The side

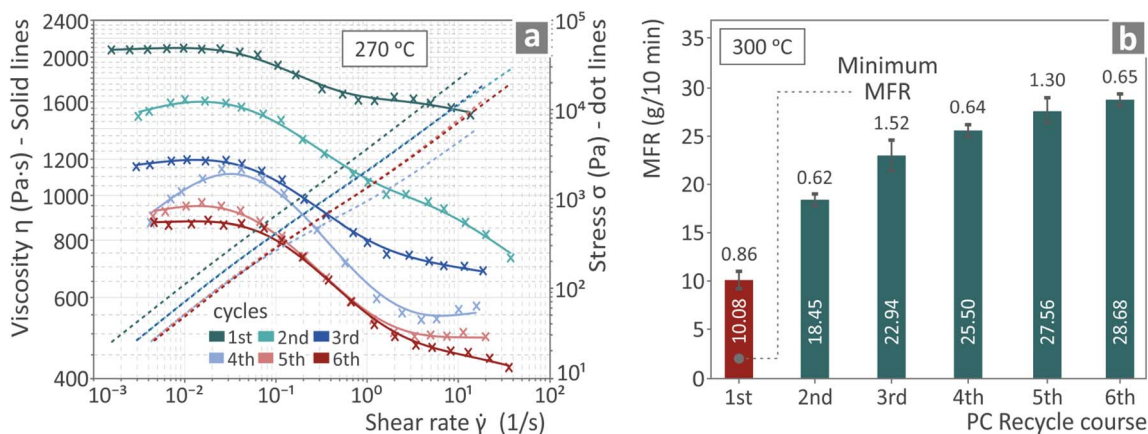


Fig. 8 Results of the six PC recycling cycles, (a) graphs of viscosity vs. shear rate and stress vs. shear rate and (b) MFR.



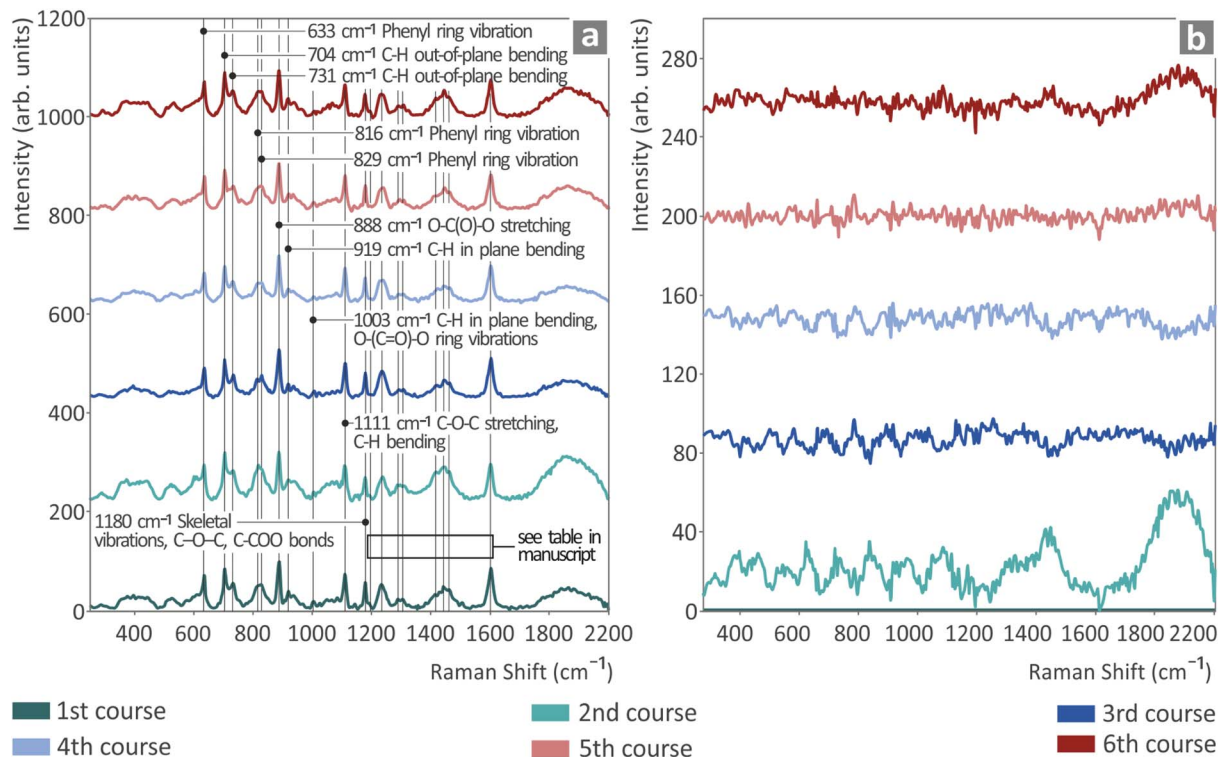


Fig. 9 (a) The graph above presents the Raman spectra of the six recycling cycles of the PC, and (b) the Raman spectral differences of the third to sixth recycling cycle of the PC.

surface layering shows a non-uniform layering, still, the layers' fusion seems solid. This should have contributed to the good mechanical performance of the samples of the specific cycle (highest tensile strength). Voids and defects in the layer formation appear. Their effect on the mechanical performance is not high enough, taking into account the respective experimental results.

### 3.6 Structural examination

Fig. 12a presents, in color-coding mapping, the dimensional deviation of all the CT scan samples from every recycling cycle, along with graphs representing the related surface and deviating point *versus* the dimensional deviation. Fig. 12b and c present sections of the CT scan samples of the first and second recycling cycles, respectively, which once more display the

Table 2 Raman spectra: significant peaks of the PC samples and their related assignments

| Wavenumber ( $\text{cm}^{-1}$ ) | Intensity | Raman peak assignment   |
|---------------------------------|-----------|---|
| 633                             | Strong    | Phenyl ring vibration <sup>122,123</sup>  |
| 704                             | Strong    | C-H out-of-plane bending <sup>122</sup>   |
| 731                             | Medium    | C-H out-of-plane bending <sup>122,124</sup>   |
| 816                             | Medium    | Phenyl ring vibration <sup>123</sup>  |
| 829                             | Medium    | Phenyl ring vibration <sup>122,123</sup>  |
| 888                             | Strong    | O-C(O)-O stretching <sup>122</sup>  |
| 919                             | Small     | C-H in plane bending <sup>122,124</sup>   |
| 1003                            | Small     | C-H in plane bending; <sup>122,124</sup> O-(C=O)-O ring vibrations <sup>122</sup>         |
| 1111                            | Strong    | C-O-C stretching; <sup>122</sup> C-H bending <sup>123</sup>                               |
| 1180                            | Strong    | Skeletal vibrations, C-O-C, C-COO bond <sup>122,124-126</sup>                             |
| 1197                            | Small     | C-O-C stretch <sup>123</sup>  |
| 1235                            | Strong    | C-O-C group asymmetric vibration <sup>122,123</sup>                                       |
| 1290                            | Small     | C-O-C stretching <sup>124</sup>   |
| 1306                            | Small     | C-O-C stretching <sup>124</sup>   |
| 1417                            | Strong    | CH <sub>3</sub> deformation <sup>124</sup>  |
| 1444                            | Strong    | CH <sub>3</sub> deformation <sup>122,124</sup>  |
| 1462                            | Strong    | CH <sub>3</sub> deformation <sup>124</sup> CH <sub>3</sub> asymmetric bend <sup>123</sup> |
| 1602                            | Strong    | Phenyl ring stretch; <sup>123</sup> phenyl ring vibration <sup>124</sup>                  |



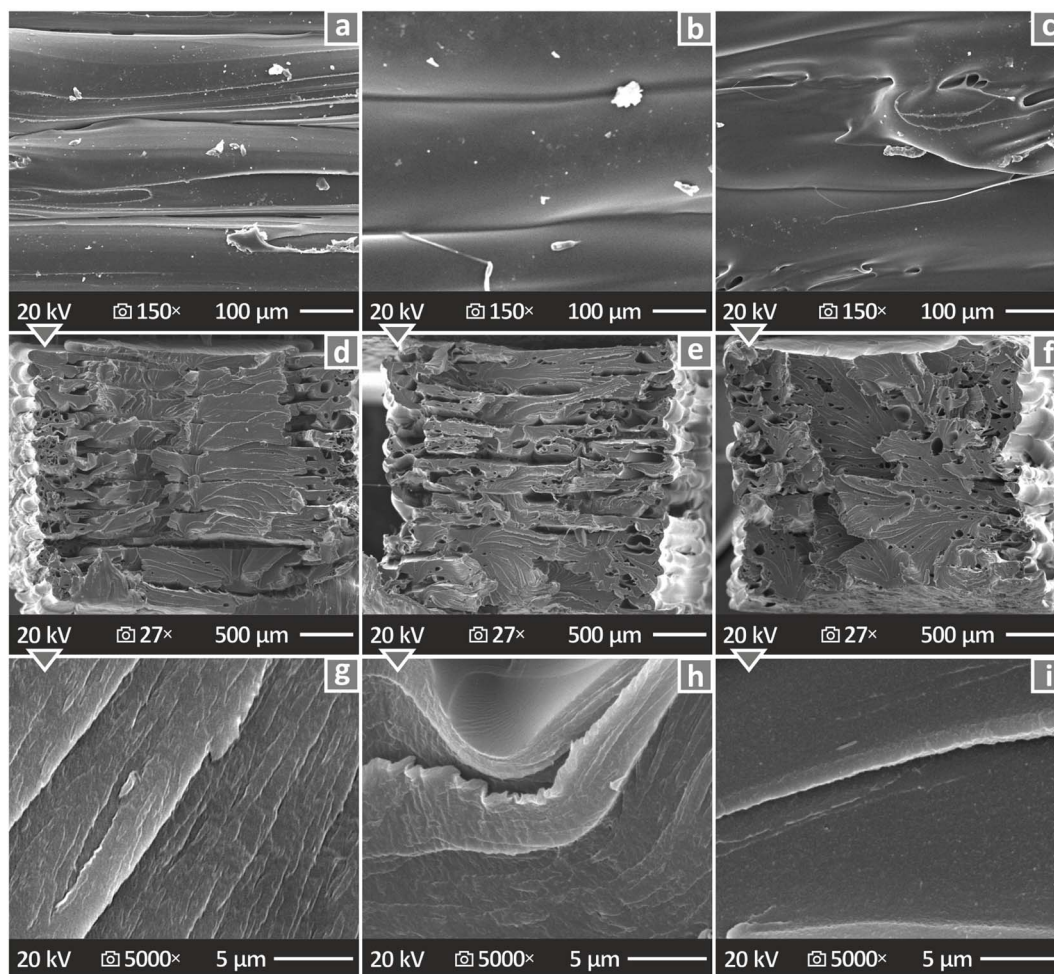


Fig. 10 (a–c) SEM images of 150 $\times$  magnification demonstrating the vertical surface of the PC first, third, and sixth samples, (d–f) SEM images of 27 $\times$  and (g–i) SEM images of 1000 $\times$  magnification demonstrating the fracture surface of the PC first, third, and sixth cycle samples.

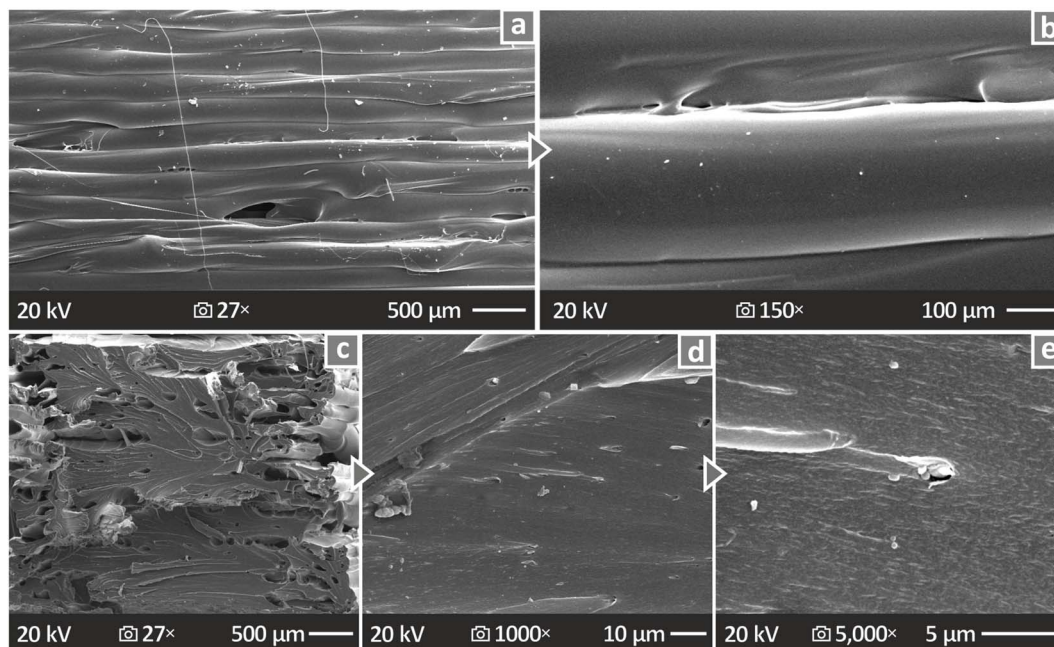


Fig. 11 (a and b) SEM image of 27 $\times$  magnification demonstrating the side surface of the PC second recycling cycle and 150 $\times$  magnification, (c–e) demonstrating an image of the fractured surface, in 27 $\times$ , 1000 $\times$  and 5000 $\times$  magnification, of the PC second recycling cycle.



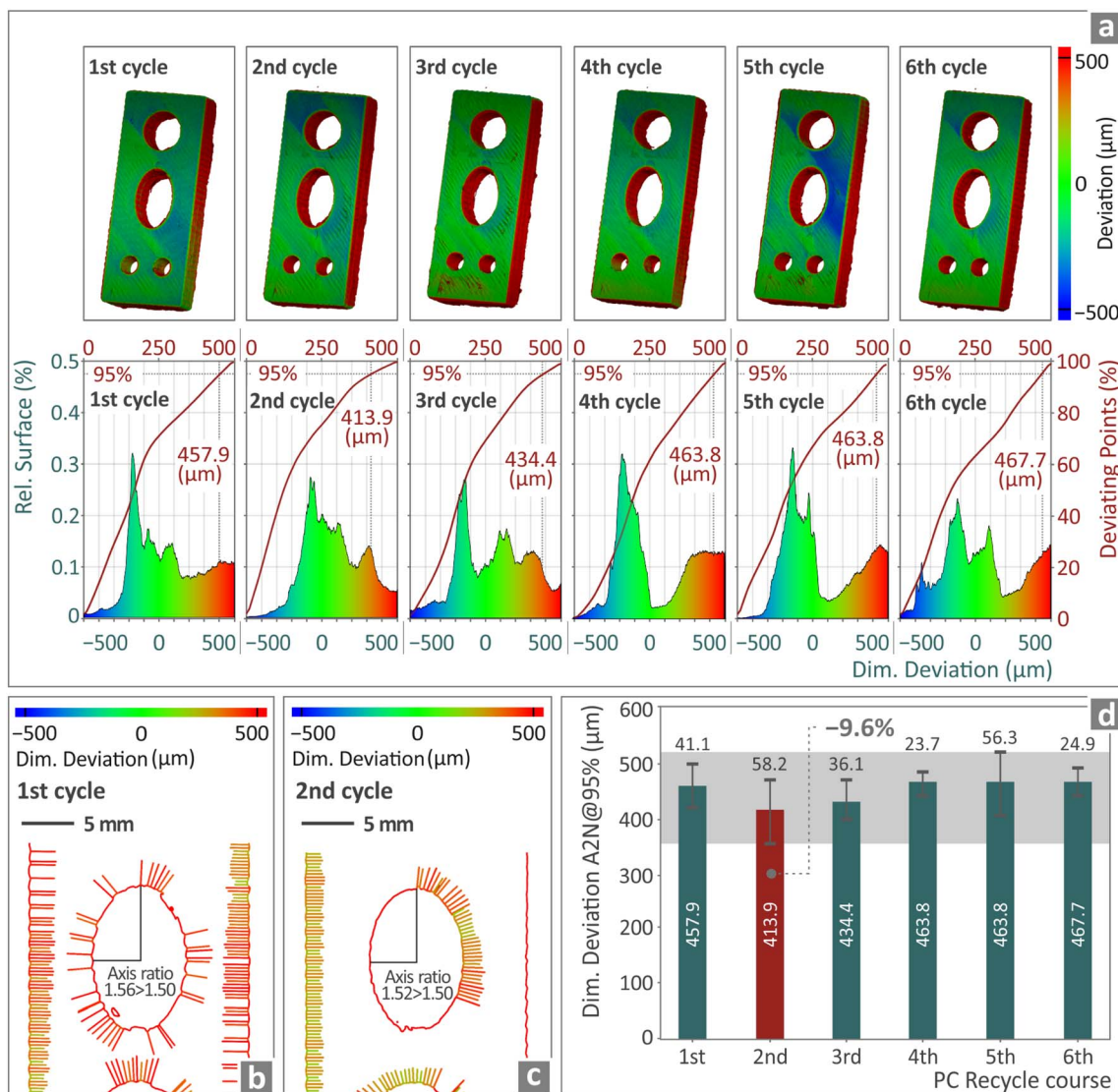


Fig. 12 (a) Color-coded mapping of the samples' dimensional deviation for each recycling cycle, including associated surface and deviating point graphs vs. dimensional deviation. (b and c) A color-coded mapping representation of sections from the first and second PC recycling cycles' dimensional deviation and (d) the levels of all PC recycling cycles' dimensional deviation.

dimensional variation using color-coding mapping. In the middle of the sample designed for the dimensional accuracy evaluation, an ellipse was formed, to increase the complexity of the shape. In Fig. 12b and c, the geometrical deviation of the horizontal and the vertical axes of the elliptical shape is presented, as determined by the  $\mu$ -CT scanning process. All of the PC recycling cycles' dimensional deviation A2N@95% levels are displayed in Fig. 12d, which also reveals that the second-course sample levels were increased by 9.6% over the first course.

Fig. 13a displays the void volume graphs *versus* the void diameter, void compactness, and void sphericity graphs *versus* the geometrical accuracy of the parts from every PC recycling cycle. Fig. 13b and c show the void volume once more using color-coding mapping. The porosity levels of all PC recycling cycles are shown in Fig. 13d, and it is evident that the second-course sample levels were 13.8% lower than the first. Beyond

the second course, the porosity constantly increased in the samples and it was higher than the virgin material samples beyond the 4<sup>th</sup> repetition.

## 4. Discussion

The aim of the research conducted was to evaluate the response of the multiple reprocessed PC in MEX 3D printing. Specifically, the polymer was processed six times. From the results, it appears that the samples from the third cycle had the best tensile properties, with a 9% increase over the first cycle. The flexural results presented the second cycle as the one with the highest properties (~14% increase in the flexural strength), while the Charpy impact results showed the best behavior of the material in the fourth cycle. The DMA results for all PC recycling cycles provided information regarding the loss and storage



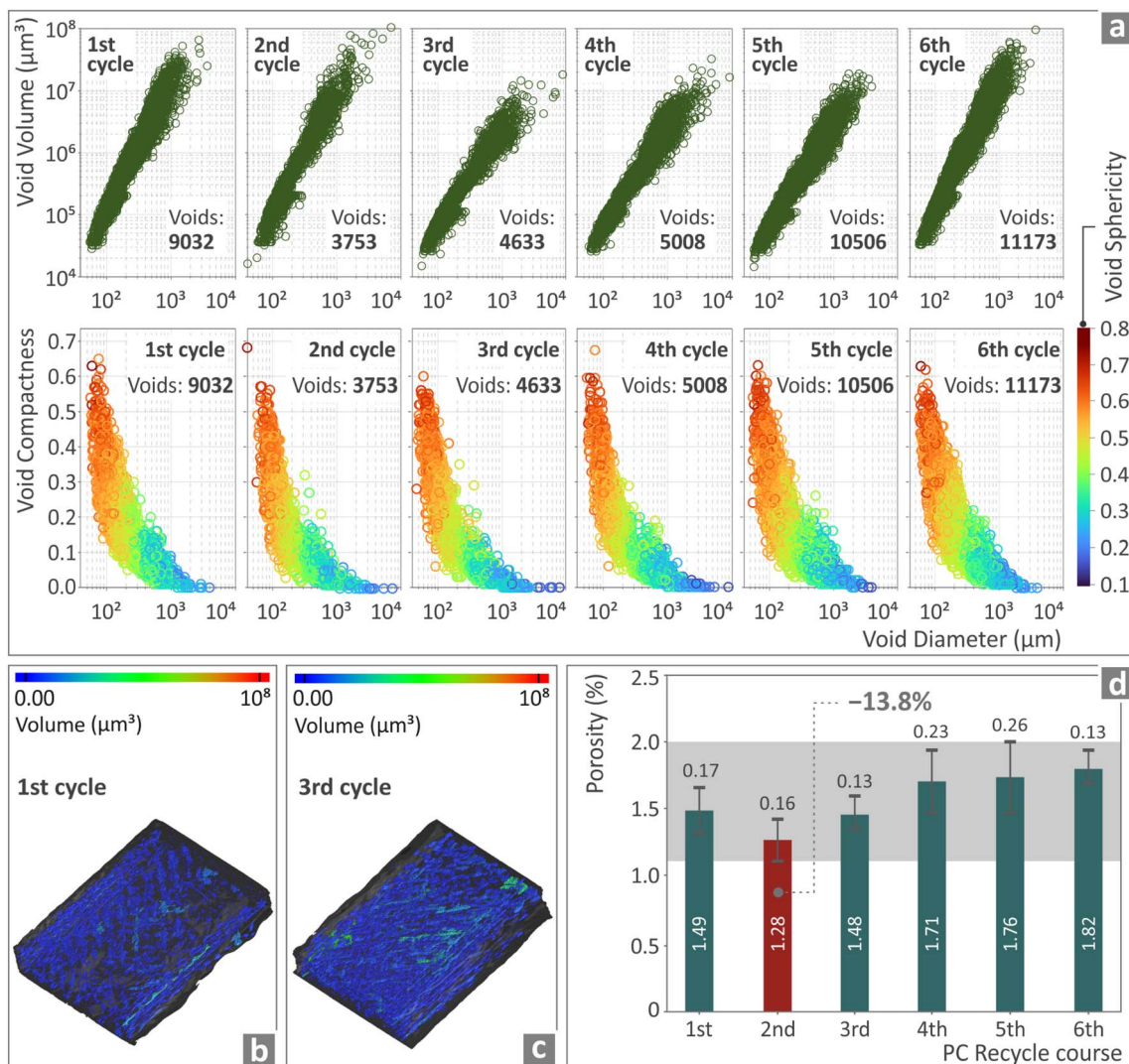


Fig. 13 (a) Graphs of the samples of each PC recycling cycle, presenting the void volume versus void diameter and void sphericity in relation to void diameter, (b and c) color-coded mapping presentation of sections of the first and third cycles of the PC recycling cycle volume, and (d) porosity levels of all PC recycling cycles.

modulus,  $\tan(\delta)$ , and flexural modulus. The  $T_g$  temperature calculated for the material of the first cycle was in good agreement with the respective DSC results. Overall, the second cycle PC material can be considered the one with the highest mechanical response, as the flexural strength and modulus are the highest among the samples tested, while the tensile strength is also high. The increase in the mechanical strength of polymers after reprocessing is an expected outcome and can be attributed to crystallization,<sup>116</sup> molecular alignment,<sup>113–115</sup> and reduction of defects.<sup>117</sup>

The enhancement in the mechanical properties of recycled polycarbonate (PC) during specific recycling cycles in MEX 3D printing can be attributed to several interrelated factors. Initially, the recycling process may alleviate residual stresses and promote improved polymer chain alignment, resulting in increased material uniformity. These modifications can enhance interlayer cohesion and print densification, thereby

improving tensile strength and stiffness. Additionally, limited chain scission during early recycling slightly reduces molecular weight, leading to decreased melt viscosity and improved flow behavior, which in turn enhances layer fusion and print quality. This was verified in the MFR test, in which MFR increased with the increase of the recycling courses. An increase in the melt flow index (MFI) indicates that the polymer flows more easily and has a lower viscosity. However, such enhancements are confined to the initial recycling stages; beyond a certain point, further degradation results in excessive chain scission, oxidation, and loss of molecular integrity, ultimately diminishing mechanical properties. Therefore, the observed improvement in mechanical performance during one recycling cycle likely results from a balance between structural relaxation, improved processability, and preserved molecular weight before significant polymer degradation occurs after multiple successive thermomechanical courses. Herein, beyond the third



reprocessing repetition the mechanical properties start to constantly decrease.<sup>127,128</sup>

It should be noted that the microhardness decreased as the recycling repetitions increased, while the stiffness of the material also decreased (Young's and flexural modulus, beyond the second recycling course). This shows that the thermo-mechanical reprocessing of the PC thermoplastic initially increases its strength and then it is decreased, while it makes it more soft and less stiff.

Regarding the thermal properties, TGA revealed no significant differences in the temperature, in which the samples from the different cycles start to degrade. The final residue also did not show notable differences between the examples from the six cycles. The  $IDT_{@95\%}$  remained steady (deviation <1%) throughout all recycling cycles. The FR of samples 2–6 is lower than that of the first cycle because of the lower molecular weight, and hence, lower molecular stability.<sup>129</sup> However, the FR of samples 2–6 fluctuates. This can be attributed to impurities or other additives that can be introduced during recycling and alter the thermal behavior of the polymer.

In the DSC analysis, as mentioned, the glass transition temperature ( $T_g$ ) of the recycled samples did not change significantly (<3%) but slightly decreased with each recycling cycle. This reduction in  $T_g$  occurs because of the degradation and scission of the polymer chains during the recycling process, leading to a decrease in the molecular weight and chain entanglement, as mentioned earlier. Shorter molecular chains have higher mobility than longer chains, which makes the transition from a rigid state to glassy state easier at a slightly lower temperature.<sup>130</sup> Furthermore, the aforementioned

impurities can act as plasticizers, enhancing the chain mobility and contributing to the decrease in  $T_g$ .

Regarding the MFR results, the first recycling cycle of the PC samples had the lowest levels, which appeared to increase as the recycling process proceeded. This agrees with the viscosity results, in which the viscosity reduces with the increase of the number of thermomechanical reprocessing on the PC polymer. Practically, this means that the material flows more easily. This instructs an adjustment in the 3D printing settings for each recycling repetition, to accomplish a better 3D printing structure and as a result better mechanical response. This was not done in the experimental process, to have comparable results. The differences found in the mechanical properties between the samples from different cycles and the layer formation issues presented on the SEM illustrations of the lateral side of the samples of the sixth recycling course can be partly attributed to these differences in the rheology of the PC polymer, due to its reprocessing. Additionally, the MFR increase suggests that the molecular weight of the PC polymer lowers,<sup>119</sup> with the successive recycling courses.

The  $\mu$ -CT results showed a positive effect in the case of the second-cycle samples. These samples showed the lower porosity and the highest geometrical accuracy among the samples from the six recycling courses. This outcome indicates a correlation between these two quality metrics and the samples' mechanical strength. The ones from the second recycling course were the ones with the highest mechanical response in the research. The positive effect of reduced 3D printing structure porosity in the mechanical response of the parts is the expected outcome and agrees with the literature.<sup>131</sup>

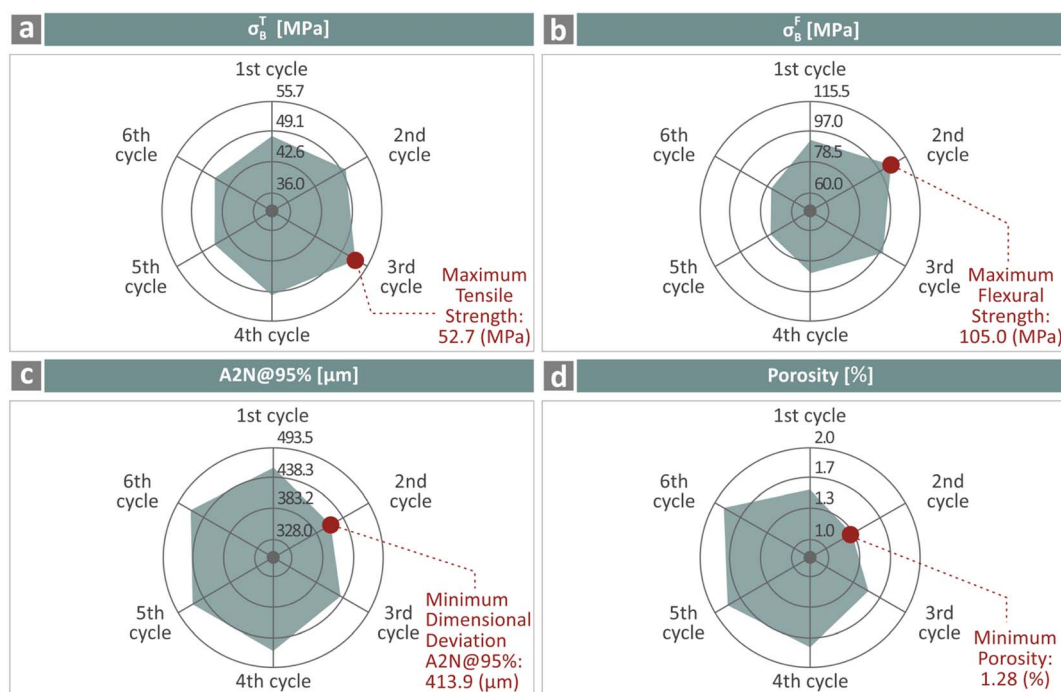


Fig. 14 Spider graphs showing the outline of the (a) strength in the tensile experiment, (b) strength in the flexural experiment, (c) A2N@95%, and (d) porosity results.



Table 3 Recycled polymers in MEX 3D printing: response in tensile tests

| Increase (%)                  | PC  | PP <sup>106</sup> | PA12 <sup>107</sup> | PETG <sup>110</sup> | HDPE <sup>108</sup> | ABS <sup>105</sup> |
|-------------------------------|-----|-------------------|---------------------|---------------------|---------------------|--------------------|
| Tensile strength              | 9.0 | ~4.0              | ~14.0               | ~14.0               | ~19.0               | ~20.0              |
| Recycling repetition achieved | 3   | 2                 | 4                   | 3                   | 4                   | 5                  |

Fig. 14 shows a summary of the tested properties in spider graphs. Specifically, the tensile and flexural strengths of the samples, A2N, and the void percentage. Along with the corresponding measured values, the PC recycling cycles that exhibited the highest and minimum levels (the focus of this research) were also highlighted.

Regarding the limitations of the research, in polymer recycling, parameters such as aging and weather conditions affect the properties of the recycled polymers.<sup>118</sup> These parameters were not considered in the research and might lead to slightly altered results. This research focused on the impact of thermomechanical reprocessing on the PC polymer properties for the exploitation of PC parts at the end of their life as raw materials for the MEX 3D printing method.

Generally, similar recycling work has been done in other polymers in MEX 3D printing, such as polypropylene (PP),<sup>106</sup> polyamide 12,<sup>107</sup> polyethylene terephthalate glycol (PETG),<sup>110</sup> HDPE,<sup>108</sup> and ABS,<sup>105</sup> as mentioned in the bibliography section of the manuscript. The rise in the mechanical properties of the polymers is not the aim of recycling. Still, this is a welcome effect. All polymers shown in Table 3 were subjected to six recycling repetitions in MEX 3D printing and proved their functionality after this experimental procedure. In Table 3, the highest improvement in their tensile strength and the cycle this occurred is presented to highlight the differences in their behavior, due to successive thermomechanical reprocessing. PP showed the lowest increase,<sup>106</sup> while ABS<sup>105</sup> showed the highest one after more recycling rounds than the other polymers. This is an indication that ABS might be more resistant to thermomechanical reprocessing than the other polymers tested and presented in Table 3.

## 5. Conclusions

This research elucidates the feasibility and advantages of polycarbonate (PC) recycling in 3D printing applications. By utilizing the recycled PC material derived originally from PC sheet scrap, we obtained mechanical properties equivalent to or higher than those of virgin PC up to the third recycling repetition. The main findings are summarized as follows:

- A ~9% rise in the strength of the parts subject to tensile testing was found in the third recycling course.
- A ~14% increase in the flexural strength in the second recycling course.
- The recycled PC filaments exhibited satisfactory printability, although minor adjustments to 3D printing parameters were necessary for effective printing.
- Challenges persist, including maintaining filament quality consistency through multiple recycling cycles.

- Up to the sixth thermomechanical reprocessing investigated, no risk of degradation during thermal reprocessing was found.

- Recycled PC demonstrates potential in MEX 3D printing for the production of prototypes and may be suitable for functional parts in applications requiring high strength, thermal resistance, and durability.

Based on our findings, we posit that enhancing selective quality assurance measures and incorporating minimal quantities of stabilizers during the recycling process would expand the potential for improved lifespan and reliability of recycled PC materials.

Future research should investigate the broader effects of PC recycling processes for 3D printing applications on lifecycle impact, particularly focusing on closed-loop systems in industrial environments. Additionally, effects, such as weathering, should be evaluated for real-life recycling applications.

## Data availability

The authors confirm that the data supporting the findings of this study are available within the article and its ESI.†

## Author contributions

Markos Petousis: methodology, formal analysis, writing—original draft preparation, writing—review, and editing; Nikolaos Michailidis: supervision, project administration, validation, methodology; Vassilis Papadakis: visualization, validation, formal analysis, data curation; Katerina Gkagkanatsiou: formal analysis, data curation, writing—original draft preparation; Apostolos Argyros: data curation, visualization; Nikolaos Mountakis: visualization, formal analysis, data curation; Vasileios Stratiotou Efstratiadis: data curation, formal analysis; Constantine David: visualization, supervision, methodology, validation; Dimitrios Sagris: validation, visualization, formal analysis; Nectarios Vidakis: conceptualization, methodology, resources, supervision, project administration. All the authors approved the final version of the manuscript.

## Conflicts of interest

The authors declare no conflicts of interest.

## Acknowledgements

The authors would like to thank the Institute of Electronic Structure and Laser of the Foundation for Research and Technology-Hellas (IESL-FORTH) and, in particular, Ms. Aleka



Manousaki for taking the SEM images presented in this work and the Photonic Phononic and Meta-Materials Laboratory for sharing the Raman Instrumentation.

## References

- B. Berman, 3-D printing: The new industrial revolution, *Bus. Horiz.*, 2012, **55**, 155–162.
- C. K. Chua, K. F. Leong and C. S. Lim, *Rapid Prototyping*, World Scientific, 2003.
- J. L. Chulilla Cano, The Cambrian Explosion of Popular 3D Printing, *Int. J. Interact. Multimed. Artif. Intell.*, 2011, **1**, 30.
- D. Espalin, D. W. Muse, E. MacDonald and R. B. Wicker, 3D Printing multifunctionality: structures with electronics, *Int. J. Adv. Manuf. Technol.*, 2014, **72**, 963–978.
- S. Rohde, J. Cantrell, A. Jerez, C. Kroese, D. Damiani, R. Gurnani, L. DiSandro, J. Anton, A. Young, D. Steinbach and P. Ifju, Experimental Characterization of the Shear Properties of 3D-Printed ABS and Polycarbonate Parts, *Exp. Mech.*, 2018, **58**, 871–884.
- S. Kumar, *Additive Manufacturing Processes*, Springer International Publishing, Cham, 2020.
- N. Shahrubudin, T. C. Lee and R. Ramlan, An Overview on 3D Printing Technology: Technological, Materials, and Applications, *Procedia Manuf.*, 2019, **35**, 1286–1296.
- I. Chiulan, A. Frone, C. Brandabur and D. Panaitescu, Recent Advances in 3D Printing of Aliphatic Polyesters, *Bioengineering*, 2017, **5**, 2.
- R. Sultan, M. Skrifvars and P. Khalili, 3D printing of polypropylene reinforced with hemp fibers: Mechanical, water absorption and morphological properties, *Heliyon*, 2024, **10**, e26617.
- S. Ganesh Sarvankar and S. N. Yewale, Additive Manufacturing in Automobile Industry.
- M. Revilla-León, M. J. Meyers, A. Zandinejad and M. Özcan, A review on chemical composition, mechanical properties, and manufacturing work flow of additively manufactured current polymers for interim dental restorations, *J. Esthetic Restor. Dent.*, 2019, **31**, 51–57.
- S. P. Dubey, V. K. Thakur, S. Krishnaswamy, H. A. Abhyankar, V. Marchante and J. L. Brighton, Progress in environmental-friendly polymer nanocomposite material from PLA: Synthesis, processing and applications, *Vacuum*, 2017, **146**, 655–663.
- N.-A. A. B. Taib, M. R. Rahman, D. Huda, K. K. Kuok, S. Hamdan, M. K. Bin Bakri, M. R. M. Bin Julaihi and A. Khan, A review on poly lactic acid (PLA) as a biodegradable polymer, *Polym. Bull.*, 2023, **80**, 1179–1213.
- M. Petousis, N. Vidakis, N. Mountakis, E. Karapidakis and A. Moutsopoulou, Functionality Versus Sustainability for PLA in MEX 3D Printing : The Impact of Generic Process Control Factors on Flexural Response and Energy Efficiency, *Polymers*, 2023, **15**, 1232.
- H. Wu, W. P. Fahy, S. Kim, H. Kim, N. Zhao, L. Pilato, A. Kafi, S. Bateman and J. H. Koo, Recent developments in polymers/polymer nanocomposites for additive manufacturing, *Prog. Mater. Sci.*, 2020, **111**, 100638.
- K. C. Chuang, J. E. Grady, R. D. Draper, C. Patterson and T. D. Santelle, Additive Manufacturing and Characterization of Ultem Polymers and Composites, in *Proceedings of the CAMX-The Composites and Advanced Materials Expo*, Atlanta, GA, USA, 2023.
- G. A. Mazzei Capote, N. M. Rudolph, P. V. Osswald and T. A. Osswald, Failure surface development for ABS fused filament fabrication parts, *Addit. Manuf.*, 2019, **28**, 169–175.
- D. J. Roach, C. Roberts, J. Wong, X. Kuang, J. Kovitz, Q. Zhang, T. G. Spence and H. J. Qi, Surface modification of fused filament fabrication (FFF) 3D printed substrates by inkjet printing polyimide for printed electronics, *Addit. Manuf.*, 2020, **36**, 101544.
- N. A. B. Nordin, M. A. Bin Johar, M. H. I. Bin Ibrahim and O. M. F. bin Marwah, Advances in High Temperature Materials for Additive Manufacturing, *IOP Conf. Ser.:Mater. Sci. Eng.*, 2017, **226**, 12176.
- A. C. de Leon, Q. Chen, N. B. Palaganas, J. O. Palaganas, J. Manapat and R. C. Advincula, High performance polymer nanocomposites for additive manufacturing applications, *React. Funct. Polym.*, 2016, **103**, 141–155.
- G. J. Schiller, in *2015 IEEE Aerospace Conference*, IEEE, 2015, pp. 1–8.
- M. Revilla-León, Metal Additive Manufacturing Technologies: Literature Review of Current Status and Prosthodontic Applications, *Int. J. Comput. Dent.*, 2019, DOI: [10.5167/UZH-184752](https://doi.org/10.5167/UZH-184752).
- C. K. Kum, Y.-T. Sung, M. S. Han, W. N. Kim, H. S. Lee, S.-J. Lee and J. Joo, Effects of morphology on the electrical and mechanical properties of the polycarbonate/multi-walled carbon nanotube composites, *Macromol. Res.*, 2006, **14**, 456–460.
- M. Petousis, I. Ntintakis, C. David, D. Sagris, N. K. Nasikas, A. Korlos, A. Moutsopoulou and N. Vidakis, A Coherent Assessment of the Compressive Strain Rate Response of PC, PETG, PMMA, and TPU Thermoplastics in MEX Additive Manufacturing, *Polymers*, 2023, **15**, 3926.
- J. de Ciurana, L. Serenóa and È. Vallès, Selecting Process Parameters in RepRap Additive Manufacturing System for PLA Scaffolds Manufacture, *Proc. CIRP*, 2013, **5**, 152–157.
- M. Kasparova, L. Grafova, P. Dvorak, T. Dostalova, A. Prochazka, H. Eliasova, J. Prusa and S. Kakawand, Possibility of reconstruction of dental plaster cast from 3D digital study models, *Biomed. Eng. Online*, 2013, **12**, 49.
- Y. He, G. Xue and J. Fu, Fabrication of low cost soft tissue prostheses with the desktop 3D printer, *Sci. Rep.*, 2014, **4**, 6973.
- M. M. Hanczyc, J. M. Parrilla, A. Nicholson, K. Yanev and K. Stoy, Creating and Maintaining Chemical Artificial Life by Robotic Symbiosis, *Artif. Life*, 2015, **21**, 47–54.
- M. Revilla-León, M. J. Meyer, A. Zandinejad and M. Özcan, Additive manufacturing technologies for processing zirconia in dental applications, *Int. J. Comput. Dent.*, 2020, **23**(1), 27–37.
- A. Arivazhagan and S. Masood, Dynamic mechanical properties of ABS material processed by fused deposition modelling, *Int. J. Eng. Res. Ind. Appl.*, 2012, **2**, 2009–2014.



- 31 V. E. Dreval, G. B. Vasil'ev, E. K. Borisenkova and V. G. Kulichikhin, Rheological and mechanical properties of ABS plastics prepared by bulk polymerization, *Polym. Sci., Ser. A*, 2006, **48**, 338–345.
- 32 H. Ramezani Dana, F. Barbe, L. Delbreilh, M. Ben Azzouna, A. Guillet and T. Breteau, Polymer additive manufacturing of ABS structure: Influence of printing direction on mechanical properties, *J. Manuf. Process.*, 2019, **44**, 288–298.
- 33 N. Vidakis, M. Petousis, D. Kalderis, N. Michailidis, E. Maravelakis, V. Saltas, N. Bolanakis, V. Papadakis, A. Argyros, N. Mountakis and M. Spiridaki, A coherent engineering assessment of ABS/biochar biocomposites in MEX 3D additive manufacturing, *Heliyon*, 2024, **10**, e32094.
- 34 S. J. Leigh, C. P. Purssell, D. R. Billson and D. A. Hutchins, Using a magnetite/thermoplastic composite in 3D printing of direct replacements for commercially available flow sensors, *Smart Mater. Struct.*, 2014, **23**, 095039.
- 35 B. Wijnen, E. J. Hunt, G. C. Anzalone and J. M. Pearce, Open-Source Syringe Pump Library, *PLoS One*, 2014, **9**, e107216.
- 36 G. Anzalone, A. Glover and J. Pearce, Open-Source Colorimeter, *Sensors*, 2013, **13**, 5338–5346.
- 37 M. Petousis, D. Sagris, V. Papadakis, A. Moutsopoulou, A. Argyros, C. David, J. Valsamos, M. Spiridaki, N. Michailidis and N. Vidakis, Optimization Course of Titanium Nitride Nanofiller Loading in High-Density Polyethylene: Interpretation of Reinforcement Effects and Performance in Material Extrusion 3D Printing, *Polymers*, 2024, **16**, 1702.
- 38 N. Guo and M. C. Leu, Additive manufacturing: technology, applications and research needs, *Front. Mech. Eng.*, 2013, **8**, 215–243.
- 39 M. Petousis, M. Spiridaki, N. Mountakis, A. Moutsopoulou, E. Maravelakis and N. Vidakis, Box-Behnken modeling to optimize the engineering response and the energy expenditure in material extrusion additive manufacturing of short carbon fiber reinforced polyamide 6, *Int. J. Adv. Manuf. Technol.*, 2024, **132**, 4399–4415.
- 40 A. Al Rashid, S. A. Khan, S. G. Al-Ghamdi and M. Koç, Additive manufacturing: Technology, applications, markets, and opportunities for the built environment, *Autom. Construct.*, 2020, **118**, 103268.
- 41 A. Paolini, S. Kollmannsberger and E. Rank, Additive manufacturing in construction: A review on processes, applications, and digital planning methods, *Addit. Manuf.*, 2019, **30**, 100894.
- 42 N. Vidakis, M. Petousis, N. Mountakis and E. Karapidakis, Box-Behnken modeling to quantify the impact of control parameters on the energy and tensile efficiency of PEEK in MEX 3D-printing, *Heliyon*, 2023, e18363.
- 43 R. Imran, A. Al Rashid and M. Koç, Review on computational modeling for the property, process, product and performance (PPPP) characteristics of additively manufactured porous magnesium implants, *Bioprinting*, 2022, **28**, e00236.
- 44 H. Ikram, A. Al Rashid and M. Koç, Synthesis and characterization of hematite ( $\alpha$ -Fe<sub>2</sub>O<sub>3</sub>) reinforced polylactic acid (PLA) nanocomposites for biomedical applications, *Compos., Part C: Open Access*, 2022, **9**, 100331.
- 45 A. Camposeo, L. Persano, M. Farsari and D. Pisignano, Additive Manufacturing: Applications and Directions in Photonics and Optoelectronics, *Adv. Opt. Mater.*, 2019, **7**, 1800419.
- 46 B. Yilmaz, A. Al Rashid, Y. A. Mou, Z. Evis and M. Koç, Bioprinting: A review of processes, materials and applications, *Bioprinting*, 2021, **23**, e00148.
- 47 S. C. Ligon, R. Liska, J. Stampfl, M. Gurr and R. Mülhaupt, Polymers for 3D Printing and Customized Additive Manufacturing, *Chem. Rev.*, 2017, **117**, 10212–10290.
- 48 V. G. Gokhare, D. Raut and D. Shinde, A review paper on 3D-printing aspects and various processes used in the 3D-printing, *Int. J. Eng. Res. Technol.*, 2017, **6**, 953–958.
- 49 L. Xinhua, L. Shengpeng, L. Zhou, Z. Xianhua, C. Xiaohu and W. Zhongbin, An investigation on distortion of PLA thin-plate part in the FDM process, *Int. J. Adv. Manuf. Technol.*, 2015, **79**, 1117–1126.
- 50 L. Xinhua, L. Shengpeng, L. Zhou, Z. Xianhua, C. Xiaohu and W. Zhongbin, An investigation on distortion of PLA thin-plate part in the FDM process, *Int. J. Adv. Manuf. Technol.*, 2015, **79**, 1117–1126.
- 51 D. Popescu, A. Zapciu, C. Amza, F. Baciuc and R. Marinescu, FDM process parameters influence over the mechanical properties of polymer specimens: A review, *Polym. Test.*, 2018, **69**, 157–166.
- 52 X. Zhou, Y. Zhai, K. Ren, Z. Cheng, X. Shen, T. Zhang, Y. Bai, Y. Jia and J. Hong, Life cycle assessment of polycarbonate production: Proposed optimization toward sustainability, *Resour., Conserv. Recycl.*, 2023, **189**, 106765.
- 53 C. Alexander and J. Reno, *Economies of Recycling: The Global Transformation of Materials, Values and Social Relations*, Bloomsbury Publishing, 2012.
- 54 Y. Liu, H. Zhou, J. Guo, W. Ren and X. Lu, Completely Recyclable Monomers and Polycarbonate: Approach to Sustainable Polymers, *Angew. Chem., Int. Ed.*, 2017, **56**, 4862–4866.
- 55 H. Shent, R. J. Pugh and E. Forssberg, A review of plastics waste recycling and the flotation of plastics, *Resour., Conserv. Recycl.*, 1999, **25**, 85–109.
- 56 A. Pegoretti, J. Kolarik and M. Slouf, Phase structure and tensile creep of recycled poly(ethylene terephthalate)/short glass fibers/impact modifier ternary composites, *EXPRESS Polym. Lett.*, 2009, **3**, 235–244.
- 57 S. M. Al-Salem, P. Lettieri and J. Baeyens, Recycling and recovery routes of plastic solid waste (PSW): A review, *Waste Manage.*, 2009, **29**, 2625–2643.
- 58 O. Sam-Daliri, T. Flanagan, V. Modi, W. Finnegan, N. Harrison and P. Ghabezi, Composite upcycling: An experimental study on mechanical behaviour of injection moulded parts prepared from recycled material extrusion printed parts, previously prepared using glass fibre polypropylene composite industry waste, *J. Cleaner Prod.*, 2025, **499**, 145280.



- 59 I. Standard, *Environmental Management-Life Cycle Assessment-Requirements and Guidelines*, ISO, 2006.
- 60 R. A. Sheldon, Metrics of Green Chemistry and Sustainability: Past, Present, and Future, *ACS Sustain. Chem. Eng.*, 2018, **6**, 32–48.
- 61 V. Krivtsov, P. A. Wäger, P. Dacombe, P. W. Gilgen, S. Heaven, L. M. Hilty and C. J. Banks, Analysis of energy footprints associated with recycling of glass and plastic—case studies for industrial ecology, *Ecol. Modell.*, 2004, **174**, 175–189.
- 62 H. H. Khoo, LCA of plastic waste recovery into recycled materials, energy and fuels in Singapore, *Resour., Conserv. Recycl.*, 2019, **145**, 67–77.
- 63 L. Ye, C. Qi, J. Hong and X. Ma, Life cycle assessment of polyvinyl chloride production and its recyclability in China, *J. Cleaner Prod.*, 2017, **142**, 2965–2972.
- 64 P. Loubet, J. Couturier, R. Horta Arduin and G. Sonnemann, Life cycle inventory of plastics losses from seafood supply chains: Methodology and application to French fish products, *Sci. Total Environ.*, 2022, **804**, 150117.
- 65 K. Cao, X. Ma, B. Zhang, Y. Wang and Y. Wang, Tensile behavior of polycarbonate over a wide range of strain rates, *Mater. Sci. Eng., A*, 2010, **527**, 4056–4061.
- 66 S. Ibrahim, A. A. Al Jaafari and A. S. Ayesh, Physical characterizations of three phase polycarbonate nanocomposites, *J. Plast. Film Sheeting*, 2011, **27**, 275–291.
- 67 S. Fukuoka, I. Fukawa, T. Adachi, H. Fujita, N. Sugiyama and T. Sawa, Industrialization and Expansion of Green Sustainable Chemical Process: A Review of Non-phosgene Polycarbonate from CO<sub>2</sub>, *Org. Process Res. Dev.*, 2019, **23**, 145–169.
- 68 A. Bahar, S. Belhabib, S. Guessasma, F. Benmahiddine, A. E. A. Hamami and R. Belarbi, Mechanical and Thermal Properties of 3D Printed Polycarbonate, *Energies*, 2022, **15**, 3686.
- 69 E. V. Antonakou and D. S. Achilias, Recent Advances in Polycarbonate Recycling: A Review of Degradation Methods and Their Mechanisms, *Waste Biomass Valorization*, 2013, **4**, 9–21.
- 70 P. Krawczak, Plastics' key role in energy-efficient building, *eXPRESS Polym. Lett.*, 2009, **3**, 752.
- 71 A. V. Krishnan, P. Stathis, S. F. Permuth, L. Tokes and D. Feldman, Bisphenol-A: an estrogenic substance is released from polycarbonate flasks during autoclaving, *Endocrinology*, 1993, **132**, 2279–2286.
- 72 S.-J. Chiu, S.-H. Chen and C.-T. Tsai, Effect of metal chlorides on thermal degradation of (waste) polycarbonate, *Waste Manage.*, 2006, **26**, 252–259.
- 73 G. Gómez-Gras, M. D. Abad and M. A. Pérez, Mechanical Performance of 3D-Printed Biocompatible Polycarbonate for Biomechanical Applications, *Polymers*, 2021, **13**, 3669.
- 74 R. Balart, L. Sánchez, J. López and A. Jiménez, Kinetic analysis of thermal degradation of recycled polycarbonate/acrylonitrile–butadiene–styrene mixtures from waste electric and electronic equipment, *Polym. Degrad. Stab.*, 2006, **91**, 527–534.
- 75 M. C. Delpech, F. M. B. Coutinho and M. E. S. Habibe, Bisphenol A-based polycarbonates: characterization of commercial samples, *Polym. Test.*, 2002, **21**, 155–161.
- 76 J. Katajisto, T. T. Pakkanen, T. A. Pakkanen and P. Hirva, *Ab initio* study on thermal degradation reactions of polycarbonate, *J. Mol. Struct.: THEOCHEM*, 2003, **634**, 305–310.
- 77 F. Liu, L. Li, S. Yu, Z. Lv and X. Ge, Methanolysis of polycarbonate catalysed by ionic liquid [Bmim][Ac], *J. Hazard. Mater.*, 2011, **189**, 249–254.
- 78 N. R. Jesudoss Hynes, R. Sankaranarayanan and J. A. Jennifa Sujana, A decision tree approach for energy efficient friction riveting of polymer/metal multi-material lightweight structures, *J. Cleaner Prod.*, 2021, **292**, 125317.
- 79 T. Sai, S. Ran, S. Huo, Z. Guo, P. Song and Z. Fang, Sulfonated Block Ionomers Enable Transparent, Fire-Resistant, Tough yet Strong Polycarbonate, *Chem. Eng. J.*, 2022, **433**, 133264.
- 80 *Polycarbonate Market-Global Industry Analysis, Size, Share, Growth, Trends and Forecast, 2022-2031*.
- 81 *GVR Report cover Polycarbonate Market Size, Share & Trends Analysis Report By Application (Automotive & Transportation, Electrical & Electronics, Construction, Packaging, Consumer Goods), By Region, And Segment Forecasts, 2023-2030*.
- 82 *Polycarbonate Market Size, Share & Industry Analysis, By Grade (Standard Purpose Grade, Flame Retardant Grade, Medical Grade, Food Grade, and Others), By Application (Electrical, Construction, Packaging, Automotive, Medical Equipment, and Others), and Regional Forecast, 2024-2032*, <https://www.fortunebusinessinsights.com/polycarbonate-market-108509>.
- 83 *Global Recycled Polycarbonate Market By Type (Post Industrial Resin, Post Consumer Resin), By Application (Building Construction, Automobile), By Geographic Scope And Forecast, 2024*.
- 84 *Polycarbonate Market Size, Share, and Trends 2024 to 2033*.
- 85 *Polycarbonate Market Size by Grades (Extrusion, Injection Molding, and Others), Type (Film, Sheets, Foil, Plates, Strip, and Others), Application (Automotive Packaging, Medical, Consumer Goods, Optical Media, Electrical and Electronics), Regions, Global Industry Analysis, Share, Growth, Trends, and Forecast 2022 to 2030, 2022*.
- 86 E. V. Antonakou and D. S. Achilias, Recent Advances in Polycarbonate Recycling: A Review of Degradation Methods and Their Mechanisms, *Waste Biomass Valorization*, 2013, **4**, 9–21.
- 87 S. Kahlen, G. M. Wallner and R. W. Lang, Aging behavior and lifetime modeling for polycarbonate, *Sol. Energy*, 2010, **84**, 755–762.
- 88 J. Shea, E. Nelson and R. Cammons, Effect of recycling on the properties of injection molded polycarbonate, *Tech. Pap. - Soc. Plast. Eng.*, 1975, **21**, 614–617.
- 89 F. Ronkay, Effect of recycling on the rheological, mechanical and optical properties of polycarbonate, *Acta Polytech. Hung.*, 2013, **10**, 209–220.



- 90 Z. Zhang, F. Xu, Y. Zhang, C. Li, H. He, Z. Yang and Z. Li, A non-phosgene process for bioderived polycarbonate with high molecular weight and advanced property profile synthesized using amino acid ionic liquids as catalysts, *Green Chem.*, 2020, **22**, 2534–2542.
- 91 D. Xing, L. Lu, K. S. Teh, Z. Wan, Y. Xie and Y. Tang, Highly flexible and ultra-thin Ni-plated carbon-fabric/polycarbonate film for enhanced electromagnetic interference shielding, *Carbon*, 2018, **132**, 32–41.
- 92 J. G. Kim, Chemical recycling of poly(bisphenol A carbonate), *Polym. Chem.*, 2020, **11**, 4830–4849.
- 93 L. d. M. Lacerda, A. O. Nunes, J. M. F. de Paiva and V. A. d. S. Moris, Avaliação dos impactos ambientais de um processo industrial utilizando como matéria-prima policarbonatos virgem e reciclado, *Eng. Sanitária Ambient.*, 2019, **24**, 1103–1113.
- 94 H. W. Kua and Y. Lu, Environmental impacts of substituting tempered glass with polycarbonate in construction – An attributional and consequential life cycle perspective, *J. Cleaner Prod.*, 2016, **137**, 910–921.
- 95 K. B. Abbàs, Reprocessing of thermoplastics. II. Polycarbonate, *Polym. Eng. Sci.*, 1980, **20**, 376–382.
- 96 J. Zhang, A. Panwar, D. Bello, J. A. Isaacs, T. Jozokos and J. Mead, The effects of recycling on the structure and properties of carbon nanotube-filled polycarbonate, *Polym. Eng. Sci.*, 2018, **58**, 1278–1284.
- 97 J. M. Pérez, J. L. Vilas, J. M. Laza, S. Arnáiz, F. Mijangos, E. Bilbao, M. Rodríguez and L. M. León, Effect of reprocessing and accelerated ageing on thermal and mechanical polycarbonate properties, *J. Mater. Process. Technol.*, 2010, **210**, 727–733.
- 98 C. A. Bernardo, A. M. Cunha and M. J. Oliveira, The recycling of thermoplastics: Prediction of the properties of mixtures of virgin and reprocessed polyolefins, *Polym. Eng. Sci.*, 1996, **36**, 511–519.
- 99 N. Vidakis, M. Petousis, C. N. David, D. Sagris, N. Mountakis and E. Karapidakis, Mechanical Performance over Energy Expenditure in MEX 3D Printing of Polycarbonate : A Multiparametric Optimization with the Aid of Robust Experimental Design, *J. Manuf. Mater. Process.*, 2023, **7**, 38.
- 100 N. Vidakis, M. Petousis and J. D. Kechagias, A comprehensive investigation of the 3D printing parameters' effects on the mechanical response of polycarbonate in fused filament fabrication, *Prog. Addit. Manuf.*, 2022, **7**, 713–722.
- 101 N. Vidakis, M. Petousis, P. Mangelis, E. Maravelakis, N. Mountakis, V. Papadakis, M. Neonaki and G. Thomadaki, Thermomechanical Response of Polycarbonate/Aluminum Nitride Nanocomposites in Material Extrusion Additive Manufacturing, *Materials*, 2022, **15**, 8806.
- 102 M. Petousis, N. Vidakis, N. Mountakis, S. Grammatikos, V. Papadakis, C. N. David, A. Moutsopoulou and S. C. Das, Silicon Carbide Nanoparticles as a Mechanical Boosting Agent in Material Extrusion 3D-Printed Polycarbonate, *Polymers*, 2022, **14**, 1–20.
- 103 N. Vidakis, M. Petousis, S. Grammatikos, V. Papadakis, A. Korlos and N. Mountakis, High Performance Polycarbonate Nanocomposites Mechanically Boosted with Titanium Carbide in Material Extrusion Additive Manufacturing, *Nanomaterials*, 2022, **12**, 1068.
- 104 S. J. Park, J. E. Lee, H. B. Lee, J. Park, N.-K. Lee, Y. Son and S.-H. Park, 3D printing of bio-based polycarbonate and its potential applications in ecofriendly indoor manufacturing, *Addit. Manuf.*, 2020, **31**, 100974.
- 105 N. Vidakis, M. Petousis, A. Maniadi, E. Koudoumas, A. Vairis and J. Kechagias, Sustainable Additive Manufacturing: Mechanical Response of Acrylonitrile-Butadiene-Styrene over Multiple Recycling Processes, *Sustainability*, 2020, **12**, 3568.
- 106 N. Vidakis, M. Petousis, L. Tzounis, A. Maniadi, E. Velidakis, N. Mountakis, D. Papageorgiou, M. Liebscher and V. Mechtcherine, Sustainable additive manufacturing: Mechanical response of polypropylene over multiple recycling processes, *Sustainability*, 2021, **13**, 1–16.
- 107 N. Vidakis, M. Petousis, L. Tzounis, A. Maniadi, E. Velidakis, N. Mountakis and J. D. Kechagias, Sustainable Additive Manufacturing: Mechanical Response of Polyamide 12 over Multiple Recycling Processes, *Materials*, 2021, **14**, 1–15.
- 108 N. Vidakis, M. Petousis and A. Maniadi, Sustainable additive manufacturing: Mechanical response of high-density polyethylene over multiple recycling processes, *Recycling*, 2021, **6**, 1–14.
- 109 N. Vidakis, M. Petousis, N. Mountakis, C. N. David, D. Sagris and S. C. Das, Thermomechanical Response of Thermoplastic Polyurethane used in MEX Additive Manufacturing over Repetitive Mechanical Recycling courses, *Polym. Degrad. Stab.*, 2022, **207**, 110232.
- 110 N. Vidakis, M. Petousis, L. Tzounis, S. A. Grammatikos, E. Porfyraakis, A. Maniadi and N. Mountakis, Sustainable additive manufacturing: Mechanical response of polyethylene terephthalate glycol over multiple recycling processes, *Materials*, 2021, **14**, 1–16.
- 111 A. L. De la Colina Martínez, G. Martínez Barrera, C. E. Barrera Díaz, L. I. Ávila Córdoba, F. Ureña Núñez and D. J. Delgado Hernández, Recycled polycarbonate from electronic waste and its use in concrete: Effect of irradiation, *Constr. Build. Mater.*, 2019, **201**, 778–785.
- 112 E. Kuram, B. Ozcelik and F. Yilmaz, The effects of recycling process on thermal, chemical, rheological, and mechanical properties of PC/ABS binary and PA6/PC/ABS ternary blends, *J. Elastomers Plast.*, 2016, **48**, 164–181.
- 113 J. Hopewell, R. Dvorak and E. Kosior, Plastics recycling: challenges and opportunities, *Philos. Trans. R. Soc., B*, 2009, **364**, 2115–2126.
- 114 A. Rahimi and J. M. García, Chemical recycling of waste plastics for new materials production, *Nat. Rev. Chem.*, 2017, **1**, 0046.
- 115 A. Bata, D. Nagy and Z. Weltsch, Effect of Recycling on the Mechanical, Thermal and Rheological Properties of



- Polypropylene/Carbon Nanotube Composites, *Polymers*, 2022, **14**, 5257.
- 116 N. Vidakis, M. Petousis, A. Korlos, E. Velidakis, N. Mountakis, C. Charou and A. Myftari, Strain Rate Sensitivity of Polycarbonate and Thermoplastic Polyurethane for Various 3D Printing Temperatures and Layer Heights, *Polymers*, 2021, **13**, 2752.
- 117 SDT 650 TA Instruments.
- 118 TA instruments (DSC).
- 119 F. Ronkay, Effect of Recycling on the Rheological, Mechanical and Optical Properties of Polycarbonate, *Acta Polytech. Hung.*, 2013, **10**(1), 209–220.
- 120 M. Khak and A. S. A. Ramazani, Rheological measurement of molecular weight distribution of polymers, *e-Polym.*, 2013, **13**(1), DOI: [10.1515/epoly-2013-0120](https://doi.org/10.1515/epoly-2013-0120).
- 121 Y. Ahn and H. Kim, A study on the rheological properties and processability of polycarbonate, *J. Appl. Polym. Sci.*, 2002, **86**, 2921–2929.
- 122 C. Zimmerer, I. Matulaitiene, G. Niaura, U. Reuter, A. Janke, R. Boldt, V. Sablinskas and G. Steiner, Nondestructive characterization of the polycarbonate - octadecylamine interface by surface enhanced Raman spectroscopy, *Polym. Test.*, 2019, **73**, 152–158.
- 123 V. Resta, G. Quarta, M. Lomascolo, L. Maruccio and L. Calcagnile, Raman and Photoluminescence spectroscopy of polycarbonate matrices irradiated with different energy  $^{28}\text{Si}^+$  ions, *Vacuum*, 2015, **116**, 82–89.
- 124 B. H. Stuart, Temperature studies of polycarbonate using Fourier transform Raman spectroscopy, *Polym. Bull.*, 1996, **36**, 341–346.
- 125 M. Makarem, C. M. Lee, K. Kafle, S. Huang, I. Chae, H. Yang, J. D. Kubicki and S. H. Kim, Probing cellulose structures with vibrational spectroscopy, *Cellulose*, 2019, **26**, 35–79.
- 126 A. V. Veluthandath and P. B. Bisht, Identification of Whispering Gallery Mode (WGM) coupled photoluminescence and Raman modes in complex spectra of MoS<sub>2</sub> in Polymethyl methacrylate (PMMA) microspheres, *J. Lumin.*, 2017, **187**, 255–259.
- 127 M. J. Reich, A. L. Woern, N. G. Tanikella and J. M. Pearce, Mechanical Properties and Applications of Recycled Polycarbonate Particle Material Extrusion-Based Additive Manufacturing, *Materials*, 2019, **12**, 1642.
- 128 N. Vidakis, M. Petousis, E. Velidakis, M. Spiridaki and J. D. Kechagias, Mechanical Performance of Fused Filament Fabricated and 3D-Printed Polycarbonate Polymer and Polycarbonate/Cellulose Nanofiber Nanocomposites, *Fibers*, 2021, **9**, 74.
- 129 D. Mahanta, S. A. Dayanidhi, S. Mohanty and S. K. Nayak, Mechanical, thermal, and morphological properties of recycled polycarbonate/recycled poly(acrylonitrile-butadiene-styrene) blend nanocomposites, *Polym. Compos.*, 2012, **33**, 2114–2124.
- 130 A. Romani, M. Levi and J. M. Pearce, Recycled polycarbonate and polycarbonate/acrylonitrile butadiene styrene feedstocks for circular economy product applications with fused granular fabrication-based additive manufacturing, *Sustainable Mater. Technol.*, 2023, **38**, e00730.
- 131 T. I. Corporation, “TA Instruments (Rheometer)”.

